Aus dem Institut für Toxikologie

der Heinrich-Heine-Universität Düsseldorf

Direktor/Leiter: Prof. Dr. rer. nat. Gerhard Fritz

Establishment and Optimization of the Cultivation of Murine Precision-cut Heart and Liver Slices

Dissertation

zur Erlangung des Grades eines Doktors der Medizin der Medizinischen Fakultät der Heinrich-Heine-Universität Düsseldorf

vorgelegt von

Ahmed Emre Erbay

(2026)

Als Inauguraldissertation gedruckt mit der Genehmigung der

Medizinischen Fakultät der Heinrich-Heine-Universität Düsseldorf

gez.:

Dekan/in: Prof. Dr. med. Nikolaj Klöcker

Erstgutachter/in: Prof. Dr. rer. nat. Nicole Schupp

Zweitgutacher/in: Prof. Dr. med. Nadja Lehwald-Tywuschik

Für meine Familie, die mich immer unterstützt hat.

Parts of this work have been published:

Spruck, C., Bousejra, G., Erbay, A., Herbrich, S., Dimitriadis, A., Röntgen, Z., Roolfs, F., Mboni-Johnston, I., Fritz, G., Hammad, S., Schupp, N. (2025). *Mouse precision-cut liver and kidney slices: an optimized ex vivo model for acute toxicity testing.* bioRxiv. https://doi.org/10.1101/2025.07.21.665916

Zusammenfassung

Präzisionsschnitte sind Schnitte von vitalem Gewebe, die mit einem Schlittenmikrotom in einer definierten Schnittdicke hergestellt werden können. Zur Erforschung biologischer Prozesse stellt die *ex vivo*-Kultivierung von Präzisionsschnitten eine alternative Methode zur *in vitro*-Zellkultur, sowie zu *in vivo*-Tierversuchen dar. In dieser Arbeit wurden Präzisionsschnitte der Leber und des Herzens der Maus für einen Zeitraum von bis zu 48 Stunden kultiviert. Es wurde angestrebt, die Kulturbedingungen der Präzisionsschnitte zu charakterisieren und zu optimieren, da die anschließenden Untersuchungen eine ausreichende Vitalität der Schnitte voraussetzten. Zu diesem Zweck wurde erst der Einfluss ausgewählter Parameter in der Herstellung und Kultivierung auf die Vitalität der Präzisionsschnitte mit zwei verschiedenen Vitalitätstests evaluiert. Getestet wurden Veränderungen der Schnittdicke der Präzisionsschnitte, der Zusammensetzung des Kulturmediums sowie der Lösung, die im Schlittenmikrotom während des Schneideprozesses zur Aufbewahrung der Präzisionsschnitte verwendet wurde. Die untersuchten Veränderungen beeinflussten die Vitalität der Präzisionsschnitte nicht, was eine Vereinfachung des Protokolls ohne Qualitätsverluste ermöglichte. Weiterhin konnte beobachtet werden, dass die Zugabe von Antioxidantien zum Kulturmedium sich auf die Vitalität von Präzisionsschnitten des Herzens positiv auswirkte. Insgesamt wurde bei Präzisionsschnitten des Herzens allerdings ein rascherer Vitalitätsverlust beobachtet als bei Präzisionsschnitten der Leber. Weiterhin stellte die geringe Größe des Herzens von Mäusen eine Limitation für Präzisionsschnitte des Herzens dar. Im Folgenden fokussierte sich die Arbeit daher auf Präzisionsschnitte der Leber. Die histologische Untersuchung von Präzisionsschnitten der Leber zeigte nach 24 Stunden beginnende nekrotische Veränderungen, deutete jedoch auch auf regenerative Prozesse hin. Abschließend wurden die Präzisionsschnitte der Leber beispielhaft mit Paracetamol, Cisplatin, Isoniazid und Melatonin behandelt. Es wurde hierbei erwartet, dass sich die Präzisionsschnitte, analog zu den entsprechenden Geweben in *in vivo*-Versuchen verhalten. Diese Hypothese konnte durch die Ergebnisse gestützt werden. Zusammengefasst, deuteten die Ergebnisse darauf hin, dass die *ex vivo*-Kultivierung von Präzisionsschnitten, insbesondere von Präzisionsschnitten der Leber, eine vielversprechende Alternative darstellt, um die Reaktion von Gewebe auf Toxine zu untersuchen.

Summary

Precision-cut tissue slices can be produced from vital tissue using a special tissue slicing apparatus at a set slice thickness. The *ex vivo* cultivation of precision-cut tissue slices can be used as an alternative method to *in vitro* cell cultures and *in vivo* animal experiments in the research of biological processes. In this thesis, precision-cut tissue slices of the liver and the heart of mice were incubated for a period of up to 48 hours. It was aimed to characterize and optimize the culture conditions of the precision-cut tissue slices, as the subsequent investigations required sufficient viability of the slices. Therefore, two different viability assays were applied to assess how selected parameters influence the viability of the precision-cut tissue slices. Parameters changed included the slice thickness, the composition of the culture medium and the composition of the solution that was used in the tissue slicer during the cutting process. The assessment showed that the protocol modifications had no adverse effect on the viability of precision-cut tissue slices, allowing the process to be simplified without compromising the quality. It was also observed that the addition of antioxidants to the culture medium of precision-cut heart slices had a positive effect on their viability. However, culture of precision-cut heart slices was limited by a more rapid decrease in viability over the incubation period compared to precision-cut liver slices. Another limiting factor was the small size of the mouse heart, which restricted the number of slices that could be obtained from each organ. Therefore, the further focus of the thesis was on precision-cut liver slices. Histological examination of the precision-cut liver slices revealed necrotic changes in the slices beginning after 24 hours, while at the same time signs of regenerative cell processes were also evident. Lastly, the precision-cut liver slices were treated with the model toxins acetaminophen, cisplatin, isoniazid, and melatonin. It was expected that the precision-cut liver slices would respond to treatment in a manner analogous to the response that the tissue would have shown in *in vivo* experiments. This hypothesis was confirmed by the results. Overall, the results showed that the *ex vivo* cultivation of precision-cut tissue slices, particularly precision-cut liver slices, presents a promising alternative to study the response of the tissue to various toxins.

List of Abbreviations

% ..... *per cent*
[RNA] ..... *RNA concentration*
°C ..... *degrees Celsius*
µL ..... *microliter*
µm ..... *micrometer*
µM ..... *micromolar*
•OH ..... *hydroxyl radical*
ANOVA ..... *analysis of variance*
APAP ..... *N-acetyl-p-aminophenol, acetaminophen, paracetamol*
ATP ..... *adenosine triphosphate*
BSA ..... *bovine serum albumin*
CC BY ..... *Creative Commons Attribution license*
CDDP ..... *cis-diamminedichloroplatinum, cisplatin*
cDNA ..... *complementary deoxyribonucleic acid*
CO_2 ..... *carbon dioxide*
COX ..... *cyclooxygenase*
CTR1 ..... *copper transporter 1*
CTR2 ..... *copper transporter 2*
CYP ..... *cytochrome P450 enzyme*
Cyp1a1 ..... *Cytochrome P450 family 1 subfamily A polypeptide 1 gene*
Cyp2c29 ..... *Cytochrome P450 family 2 subfamily C polypeptide 29 gene*
Cyp2e1 ..... *Cytochrome P450 family 2 subfamily E polypeptide 1 gene*
CYP2E1 ..... *cytochrome P450 family 2 subfamily E member 1 protein*
Cyp3a11 ..... *Cytochrome P450 family 3 subfamily A polypeptide 11 gene*
DILI ..... *drug-induced liver injury*
DNA ..... *deoxyribonucleic acid*
DRZE ..... *German Reference Center for Ethics in the Life Sciences*
e.g. ..... *exempli gratia, for example*
EDTA ..... *ethylenediaminetetraacetic acid*
ER ..... *endoplasmatic reticulum*
EU ..... *European Union*
FDA ..... *U.S. Food and Drug Administration*
g ..... *gram*
G ..... *gravitational force equivalent*
Gapdh ..... *glyceraldehyde 3-phosphate dehydrogenase gene*
GSH ..... *glutathione*
Gsta3 ..... *Glutathione S-transferase alpha 3 gene*
h ..... *hour, hours*
H&E staining ..... *hematoxylin and eosin staining*
H_2O ..... *water*
H_2O_2 ..... *hydrogen peroxide*
HCl ..... *hydrochloric acid*
HEPES ..... *2-[4-(2-Hydroxyethyl)piperazin-1-yl]ethane-1-sulfonic acid*
HLA ..... *human leukocyte antigen*
HOCl ..... *hypochlorous acid*
HSCs ..... *hepatic stellate cells*
Hz ..... *Hertz*
IC_{50} ..... *half maximal inhibitory concentration*
INH ..... *isonicotinic acid hydrazide, isoniazid*
InhA ..... *enoyl-acyl carrier protein reductase*
KCl ..... *potassium chloride*
kg ..... *kilogram*
KH_2PO_4 ..... *potassium dihydrogen phosphate*

KHB ..... *Krebs-Henseleit-Buffer*
L ..... *liter*
LD_{50} ..... *median lethal dose*
LMP ..... *low melting point*
LSECs ..... *liver sinusoidal endothelial cells*
M ..... *molar*
mg ..... *milligram*
$MgSO_4*7H_2O$ ..... *magnesium sulfate heptahydrate*
min ..... *minute, minutes*
mL ..... *milliliter*
mM ..... *millimolar*
MTT ..... *3-(4,5-dimethylthiazol-2-yl)-2,5-diphenyltetrazolium bromide*
n ..... *number of biological replicates*
N ..... *number of technical replicates*
NAC ..... *N-Acetylcysteine*
NaCl ..... *sodium chloride*
NAD ..... *nicotinamide adenine dinucleotide*
$NaHCO_3$ ..... *sodium bicarbonate*
NaOH ..... *sodium hydroxide*
NAPQI ..... *N-acetyl-p-benzoquinone imine*
ng ..... *nanogram*
nm ..... *nanometer*
NO_2 ..... *nitrogen dioxide*
NSAID ..... *non-steroidal anti-inflammatory drug*
O_2 ..... *oxygen*
O_2^- ..... *superoxide*
OCT ..... *organic cation transporter*
PBS ..... *phosphate-buffered saline*
PCHS ..... *precision-cut heart slices*
PCLS ..... *precision-cut liver slices*
PCTS ..... *precision-cut tissue slices*
RNA ..... *ribonucleic acid*
RNS ..... *reactive nitrogen species*
ROS ..... *reactive oxygen species*
RT-qPCR ..... *real time quantitative polymerase chain reaction*
SD ..... *standard deviation*
Sult1c2 ..... *Sulfotransferase 1 C2 gene*
TEMPO *2,2,6,6-tetramethylpiperidine-1-oxyl*
TEMPOL *4-Hydroxy-TEMPO*, *4-Hydroxy-2,2,6,6-tetramethylpiperidin-1-oxyl*
T_H17-cell ..... *T helper 17 cell*
Tris-HCl ..... *tris(hydroxymethyl)aminomethanehydrochloride*
UDP ..... *up-and-down-procedure*
Ugt1 ..... *Uridine 5'-diphospho-glucuronosyltransferase 1 gene, UDP- glucuronosyltransferase 1 gene*
ZETT ..... *Central Institution for Animal Research and Scientific Animal Welfare*

Table of Contents

1. Introduction

Parts of this chapter have been published in our preprint (1).

1.1. Ethical principles in animal experiments

Every year, the FDA approves about 43 new drugs for clinical usage (2). To ensure safe application to patients, these drugs and many more undergo a clinical trial process consisting of three phases (3). But even before starting a clinical trial, every drug goes through preclinical testing to establish an understanding of its pharmacodynamics, pharmacokinetics, and toxicity to secure human safety (4, 5). This preclinical research includes *in vivo* animal experiments (5). To put this into perspective, the number of animals used for scientific research, testing, routine production and education purposes in the EU and Norway alone was reported to be about 7.9 million in 2020 (6). The German Reference Center for Ethics in the Life Sciences (DRZE) reported that almost 72 % of all animal experiments were conducted on mice (7).

This puts the scientific community and humanity in general in need of ethical principles guiding animal experiments. The most widely accepted of these are the '3Rs' first presented by *Russell and Burch* in 1959 (8). The '3Rs' abbreviate the three principles *Replacement*, *Reduction,* and *Refinement* (9).

Replacement is the concept of replacing animal experiments with suitable alternatives (9). Notably, this approach emphasizes *in vitro* and *in silico* alternatives (10). Unfortunately, the current technology does not enable humanity to replace animal experiments altogether (11). One alternative can be 'partial replacement' by using more non-vertebrates instead of vertebrates, since they are thought of as being unable to suffer (12). But even this is challenged by new observations of nematodes such as *C. elegans*, which indicate fear-like emotional behaviors (13).

If animals cannot be replaced, *reduction* should be sought for (14). It demands keeping the number of animals per conducted study at a minimum (9). On one hand, this can be accomplished by improving study design and the exchange of data between scientists (15). On the other hand, new models such as precision-cut tissue slices (PCTS) can help collecting more experimental data per animal.

Lastly, *refinement* states that the suffering of the animals should be avoided and minimized (9). While major thinkers, such as Immanuel Kant, still questioned the

capabilities of animals as close as in the early modern period (16), we now know that animals do feel negative emotions such as pain and distress (17) as well as positive emotions like pleasure (18). This knowledge attained by mankind emphasizes human ethical responsibilities towards animals and the importance of *refinement* as a key ethical principle.

These ethical obligations are also increasingly imposed by the legislature. While the United States passed the FDA Modernization Act 2.0, authorizing alternatives to animal experiments in drug trials, in 2022 (19), the European Union already converged upon the '3Rs' in its Directive 2010/63/EU in 2010 (20). Thus, the development of 3R-conform scientific methods becomes even more important.

1.2. Precision-cut tissue slices

Researchers have widely adopted *in vitro* cell cultures as a method of *replacement*. While *in vitro* cell cultures are an approach to estimate the ultimate biological effects, they cannot replicate the complexity of living organisms (21). PCTS bridge the gap between *in vitro* cell culture and *in vivo* animal studies (22, 23). In the past, the experimental design of studies conducted with PCTS has been referred to as either '*in vitro'* or '*ex vivo'* to reflect the complex organ structure (22, 23).

PCTS are living tissue slices that are obtained by cutting the tissue very thinly with a special instrument, the technique of which was first developed by Krumdieck et al. in 1980 (24). PCTS can be made of any solid organ and they can even be expanded to non-solid organs by embedding them in agarose (23).

PCTS contain all cell types of the tissue, which offers a key benefit compared to simple cell cultures (23). This allows interactions between the different cell types and even the extracellular matrix to take place (23). Interactions with the extracellular matrix are known to be crucial to cells to the extent that e.g. hepatocytes lose their differentiation and transcriptional activity in simple *in vitro* cultures (25).

Since one organ grants multiple PCTS that can be used on multiple experimental conditions, PCTS also provide an opportunity to reduce animal experiments. Furthermore, the *postmortem* removal of organs limits animal suffering in accordance with the principle of *refinement*.

This doctoral thesis confined itself to PCTS of murine livers and hearts.

1.3. Current state of research

1.3.1. Current methods of toxicity assessment

To guarantee human safety, preclinical drug assessment uses either *in vitro* studies in cell lines or *in vivo* models in animals (26). These drug tests search for a variety of toxic reactions ranging from skin irritation to carcinogenicity (26).

Generally, two animal species, including one rodent species, undergo testing to assess acute toxicity (26). The most widely used protocol is the 'up-and-down-procedure' (UDP). In this design, doses are increased every 48 h until the test animal dies, after which the dose is reduced again. This is repeated until the LD_{50} is estimated (27).

Chronic toxicity is tested for a period of 90 days in experimental animals (26). During this time the animals are monitored for selected parameters. At the end of the study period all tissues are examined histologically (26).

Specific organ toxicities, such as hepatotoxicity, can also be studied *in vivo* in animal models. In this case, liver biomarkers such as transaminases, alkaline phosphatase, and total bilirubin levels are measured to quantify hepatotoxicity (28). While cardiac toxicity is generally assessed via echocardiography (29).

A widespread *in vitro* alternative is the use of hepatoma cell lines such as HepG2 or HepRG (30, 31, 32). While hepatocytes constitute about 78 % of the liver (33), pure hepatocyte cultures do not reflect the physiology of the liver properly. They lack crucial interactions between other cell types and the extracellular matrix that effect the gene expression of hepatocytes (25). This is why new *in vitro* methods are emerging (32). New promising models to assess hepatotoxicity are co-cultures and three-dimensional liver microtissues (32, 34). Therefore, PCTS present a similar opportunity in toxicological research, as they include all cell types of the tissue.

1.3.2. Current uses of PCTS

PCTS can be obtained from a variety of organs and therefore have a wide spectrum. Precision-cut liver slices (PCLS) in particular were already used to replicate disease processes for alcoholic fatty liver disease, non-alcoholic fatty liver disease, liver fibrosis and cirrhosis, viral hepatitis, and hepatocellular carcinoma (35).

The possible use of PCLS in the field of toxicology is known. Older studies started to study toxic reactions of halogenated hydrocarbons, acetaminophen, aflatoxin B_1, and

endotoxins in PCLS (36). More recently, drug-induced cholestasis in PCLS of rats and humans has been induced by cholestatic drugs (37, 38). Some individual drugs such as cyclosporin A, N-acetyl-aminophenol, or deoxynivalenol have been tested toxicologically on PCLS (39, 40, 41). However, widespread use is still lacking, and further research is needed. Major limitations have been the limited incubation time of the slices and the labor intensity of the method (23).

The current use of precision-cut heart slices (PCHS) is even more limited than PCLS. Human, pig, and murine culture systems of PCHS were established in recent years (42, 43). These models have been used to study heart physiology (44) and it was even possible to replicate cardiotoxic reactions (45). However, these developments are still very new and require further research.

1.4. Anatomy and physiology of the examined organs

1.4.1. Liver anatomy and physiology

The liver is an organ that performs a variety of tasks. First and foremost, the liver controls the energy metabolism of the body (46). It has a dual blood supply from the portal vein and the hepatic artery that supplies it directly with macronutrients from the digestive system (47). From there on, it stores glucose in the form of glycogen and regulates lipogenesis, ketogenesis, and amino acid metabolism (46).

In addition to metabolizing the nutrients, the liver, being an exocrine gland of the gastrointestinal tract, helps digestion by secreting bile (47). Bile is a secretion containing bile salts and phospholipids (48). Bile salts in particular are amphiphile molecules necessary for the absorption of lipid-soluble molecules in the intestine (49).

Additionally, endogenous molecules such as heme, along with xenobiotics, undergo a biotransformation process in the liver that can be broken down into three phases (50). In phase I cytochrome P450 enzymes (CYP) introduce functional groups such as amide, carboxyl, ester, hydroxyl, or sulfhydryl groups to the molecules to increase hydrophilic properties (50, 51). In phase II acetylation, glucuronidation, glutathione conjugation, methylation, or sulfation further increase the water solubility and add a negative charge to the molecules, preventing them from passing membranes (50, 51). Phase II generally puts an end to the biological activity of the molecule (51). Phase III includes the transport across the membrane via transporters (50). This biotransformation process of the liver makes it especially relevant to the fields of pharmacology and toxicology.

Other functions include the storage and metabolism of fat-soluble vitamins, deiodination of thyroid hormones, cholesterol homeostasis, and synthesis of almost all plasma proteins (47).

In its macroanatomy, rodent livers differ from human livers. Rodent livers have a lobated architecture (52). A macroanatomical picture of a murine liver is depicted in **Figure 1**. While the term 'lobe' is used in anatomical terminology of the human liver, the liver is essentially not lobulated in structure (52). For practical purposes, the division of the liver into 8 segments by *Couinaud* already replaced the anatomic nomenclature (52).

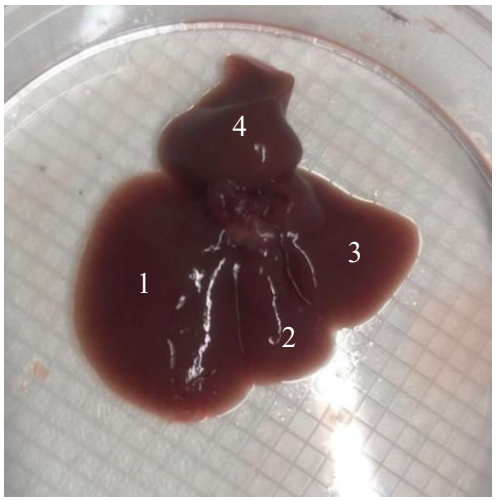

Figure 1: Macroanatomical picture of a mouse liver used in the experiments

The picture depicts exemplarily the liver of a mouse in a petri dish. The picture was taken with a smartphone camera. The depicted liver demonstrates the lobated architecture that is characteristic for murine livers. Four lobes can be identified in the liver. The lobes are numbered for better visualization.

The microscopic structure, on the other hand, is generally similar between humans and rodents (52). Most commonly, the liver is divided into liver lobules. These lobules, as worked out by *Kiernan* (53), are hexagonal in form and center around a central vein that drains the unit (54). The corners of the lobule contain branches of the triad: portal vein, hepatic artery, and bile duct (54). Sinusoids lead the blood from the portal vein and hepatic artery to the central vein (54).

Alternatively, *Mall* advocated centering the liver lobules around the bile ducts, as glandular units are usually centered around their ducts (55). These *portal units* are often seen as superior to liver lobules by hepatologists (54).

Lastly, this concept was refined to the *liver acinus* by *Rappaport* (56), to feature the terminal afferent vascular twigs and terminal bile ducts as the axes of the structural unit. According to their location within the acinus, hepatocytes are supplied with oxygen-rich or oxygen-poor blood. This allows the division of the acinus into three zones (56, 57). Hepatocytes are known to have a degree of functional specialization within these zones (58). Most notably, as for its pharmacological and toxicological relevance, most enzymes involved in xenobiotic metabolism were shown to be expressed in the perivenous zone (Zone 3) (59). In addition, a lot of hepatotoxins demonstrate zonal toxic effects (60). Ultimately, all these structural classifications can be seen as different functional units emphasizing different tasks of the liver (57). These microscopic classifications are illustrated in **Figure 2**.

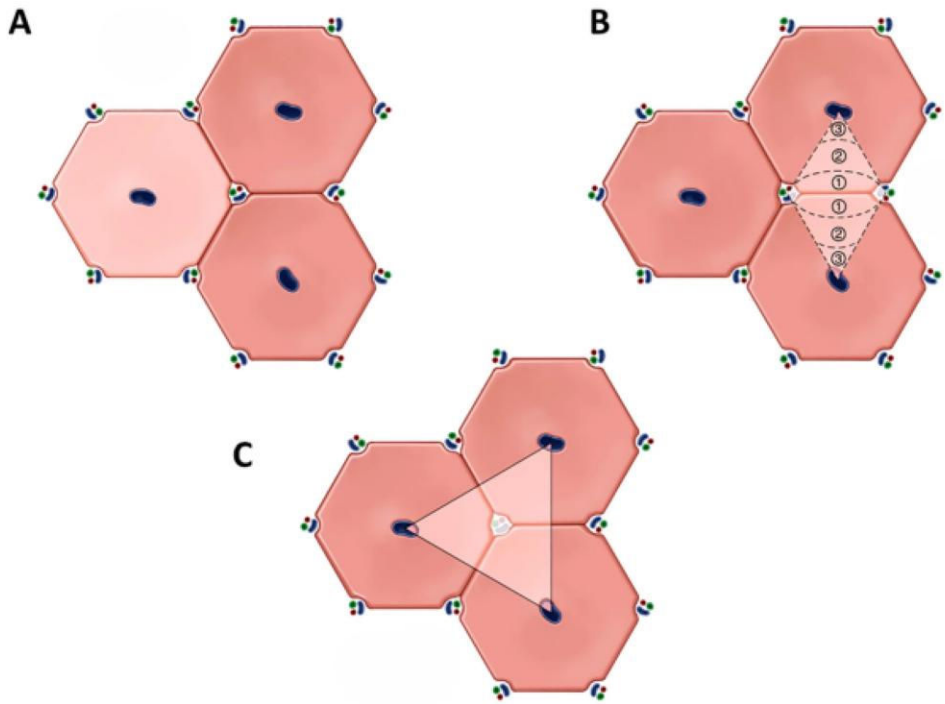

Figure 2: Microscopic architecture of the liver

The figure illustrates the three microscopic divisions of the liver. (A): Hexagonal liver lobule model by *Kiernan*. (B): Liver acinus model by *Rappaport* and their zonation overlaid on A. (C): Portal unit model by *Mall* overlaid on A. The illustration was taken and adjusted from "The Voronoi theory of the normal liver lobular architecture and its applicability in hepatic zonation" published by Lau, Kalantari, Batts et al., in 2021 (61). Licensed under CC BY 4.0.

Generally, the liver is mostly composed of hepatocytes. Early assessments estimate hepatocytes to constitute almost 80 % of the liver (62). Non-hepatocyte cell lines include endothelial cells, cholangiocytes, Kupffer cells, and hepatic stellate (Ito) cells (62). Kupffer cells are hepatic macrophages (63), while hepatic stellate (Ito) cells store Vitamin A and play a key role in fibrogenesis (64, 65). In recent years, an increasing variety of immune cells have also been described in the liver (66). The different cell types found in the liver are illustrated in **Figure 3**.

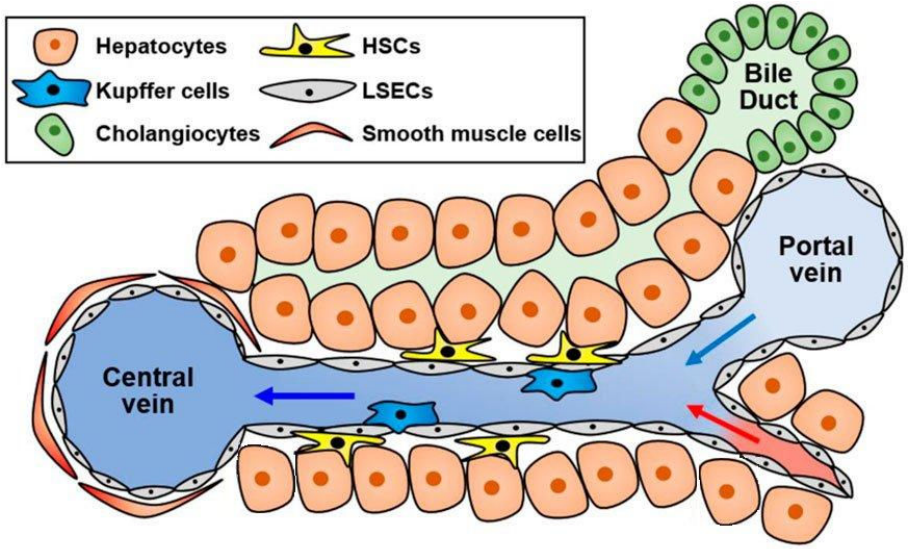

Figure 3: Cellular architecture of liver lobules highlighting the different cell types found in the liver

The figure illustrates the cellular architecture of liver lobules. The location of different cell types in the liver lobule is shown. Hepatocytes, Kupffer cells, cholangiocytes, HSCs, LSECs, and smooth muscle cells are depicted. Furthermore, the direction of blood flow from the portal vein (light blue) and the hepatic artery (red) towards the sinusoids and the central vein (dark blue) is indicated by arrows. Secreted bile that flows towards the bile ducts is shown in green. LSECs: liver sinusoidal endothelial cells, HSCs: hepatic stellate cells

The illustration was taken and adjusted from "Cellular heterogeneity and plasticity during NAFLD progression" published by Park, Choi, Kim, Yang, An, Lee, et al., in 2023 (67). Licensed under CC BY 4.0.

1.4.2. Heart anatomy and physiology

The heart is a very essential organ to the body. It maintains blood circulation throughout the body, providing oxygen to all cells of the organism. Circulation is so central to living organisms that its arrest defines clinical death, which evolves into permanent death if no resuscitation is started.

The heart is situated in the mediastinum (68). It is divided into a right and a left half, each containing one atrium and one ventricle. The atria and ventricles contract in a repeating cycle of systole and diastole. This is intensively regulated by the autonomic nervous system. During the cardiac cycle, venous blood is pumped by the right heart into the pulmonary circulation, where it becomes oxygenated. The oxygenated blood returns to the left heart and is pumped into the rest of the body. The anatomical structure of the heart is depicted in **Figure 4**.

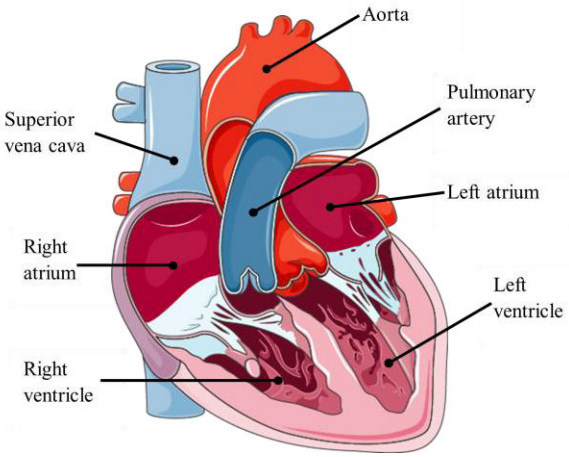

Figure 4: Diagram of heart anatomy

The diagram depicts a schematic representation of the anatomy of the heart. The image was modified and used with permission from Servier Medical Art. Licensed under CC BY 4.0.

To function properly, the heart itself is perfused by the coronary arteries. Since the heart contains only limited glycogen storage and receives its energy from the oxidation of fatty acids, it depends on a constant oxygen supply (69). Therefore, the heart is also more sensitive to ischemia (70). In cardiac surgery ischemia is prevented by cardioplegia (71). Cardioplegia is achieved by the administration of potassium which puts the heart in diastolic arrest and therefore reduces the myocardial oxygen demand (71). This is why cardioplegia was also tested on PCHS in this thesis as a way to improve their viability.

Microanatomically, the heart is mainly composed of cardiomyocytes, endothelial cells, and leukocytes (72). Recent analyses identified about 30 % of cells to be cardiomyocytes and 43 % of cells to be endothelial cells (72).

1.5. Medical Relevance

1.5.1. Drug-induced liver injury

Drug-induced liver injury (DILI) is the most common cause for acute hepatic failure in developed countries (73). It is also the most common reason for a drug being withdrawn post-marketing (74).

DILI can be divided into two subtypes. Intrinsic DILI occurs in a dose-dependent and predictable manner (75). It is caused by the hepatotoxic properties of the drug or its metabolites. Intrinsic DILI can therefore be easily replicated in animal models (75). A prominent example of this is acetaminophen toxicity (75).

Idiosyncratic DILI on the other hand, is not as predictable and dose-dependent as intrinsic DILI and has a great interindividual variation (75, 76). It is mostly determined by genetic variations (75). Suspected factors include biotransformation enzymes, mitochondria, HLA antigens, age and sex (76).

1.5.2. Drug-induced cardiotoxicity

Cardiotoxicity is a major adverse effect of anticancer drugs and antiretroviral drugs (77). Drug-induced cardiotoxicity often presents itself as an exacerbation or induction of heart failure (78). Drugs with cardiotoxic properties include most prominently anthracyclines but also cyclophosphamide, imatinib, trastuzumab, chloroquine, zidovudine, didanosine, and zalcitabine (77). In addition, numerous drugs prolong the QT interval on the electrocardiogram, which can lead to ventricular arrhythmias and sudden cardiac death (79). Therefore, drug-induced cardiotoxicity often becomes a major limiting factor in therapy. As a consequence, research in drug-induced cardiotoxicity is highly medically relevant, to which PCHS could serve as a valuable approach in researching cardiac responses to toxic agents.

1.6. Pharmacology and Toxicology of used model substances

In this thesis, the PCLS were treated with acetaminophen, cisplatin, isoniazid, and melatonin, and subsequently evaluated for their reaction. The selected drugs differed in their toxicological profiles. While acetaminophen represents a classic hepatotoxin, cisplatin acts cytotoxic across cell types, isoniazid induces toxicity only indirectly, and melatonin is generally considered non-toxic.

In addition, the antioxidants N-acetylcysteine and TEMPOL were tested on PCHS. Both compounds were applied to assess whether reducing oxidative stress improved the viability of PCHS.

1.6.1. Acetaminophen

N-acetyl-p-aminophenol (APAP) is a commonly used analgesic and antipyretic known under the name of acetaminophen in the United States or paracetamol in Europe. For simplicity, the terms ‘acetaminophen’ or ‘APAP’ will be used in this thesis.

APAP is used to manage acute and chronic pain (80). It is especially effective in mild to moderate pain and is used in combination with opioids for more severe pain (80). Its antipyretic properties are also used to reduce fever (80). Chemically, APAP is a derivative of aniline (81). The chemical structure of APAP is depicted in **Figure 5**.

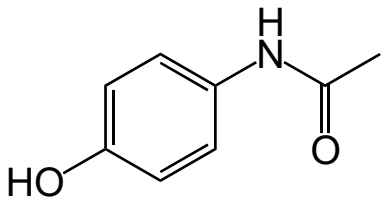

Figure 5: Chemical structure of APAP

While the mechanism of action remains unclear, it is thought to include a selective inhibition of cyclooxygenase (COX) enzymes in the central nervous system (82). This might be the reason for its selective antipyretic effects while having minimal anti-inflammatory effects (82). Its limited anti-inflammatory effect is also the reason for it being generally excluded from the non-steroidal anti-inflammatory drugs (NSAIDs) (80). Some hypotheses also include the modulation of the serotonergic system (83), the vanilloid system, or the cannabinoid system (84).

APAP is metabolized in the liver. It mostly undergoes phase II biotransformation with conjugation of glucuronic acid and sulfate (84). A smaller fraction is metabolized by the CYP450 enzymes to N-acetyl-*p*-benzoquinone imine (NAPQI). The chemical structure of NAPQI is depicted in **Figure 6**.

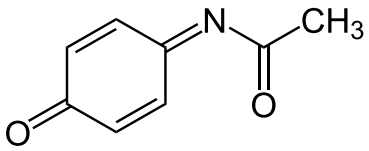

Figure 6: Chemical structure of NAPQI

NAPQI is known to bind mitochondrial proteins covalently and cause oxidative and nitrosative stress (85, 86). NAPQI also inhibits complex II of the mitochondrial respiration, decreasing ATP production (85). The mitochondrial oxidative and nitrosative stress causes necrosis with subsequent inflammatory responses (87, 88). In addition to the mitochondrial stress caused by NAPQI, ROS and covalent protein-adducts are also formed in other cellular compartments, such as the endoplasmatic reticulum (89). Overall, mitochondrial and endoplasmic reticulum (ER) stress result in DNA fragmentation (88). Under normal circumstances, glutathione (GSH) binds NAPQI before causing serious damage (86). But in the context of APAP overdosing, the phase II enzymes become saturated and GSH becomes depleted, enabling the toxic effects of NAPQI (86). The mechanism of APAP toxicity is illustrated in **Figure 7**.

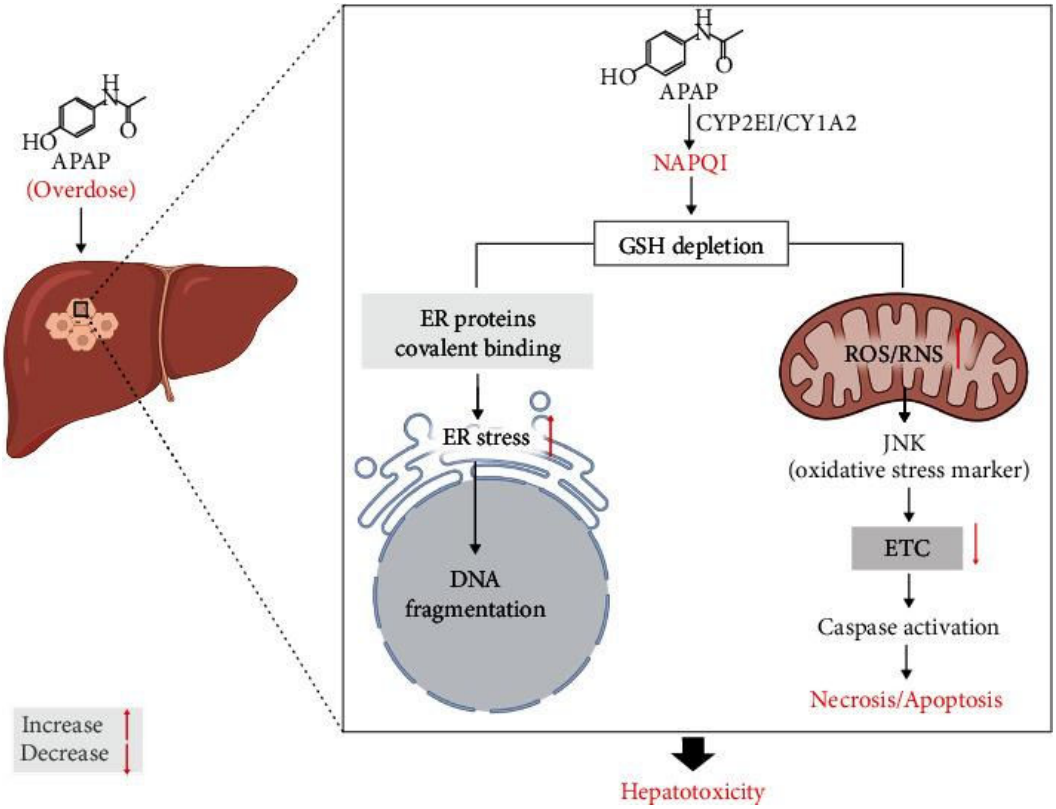

Figure 7: Illustration of APAP hepatotoxicity

Schematic illustration of the pathogenesis of APAP hepatotoxicity. In the case of APAP overdose, NAPQI is formed by CYP2E1, CYP1A2. NAPQI causes depletion of GSH in hepatocytes. The resulting ROS/RNS in mitochondria causes an increase in JNK (oxidative stress marker) and disruption in the ETC. ER stress and mitochondrial stress result in DNA fragmentation and necrosis/apoptosis. APAP: acetaminophen, NAPQI: N-acetyl-p-benzoquinone imine, CYP2E1: cytochrome P450 2E1, CYP1A2: cytochrome P450 1A2, GSH: glutathione, ER: endoplasmic reticulum, ROS/RNS: reactive oxygen/nitrogen species, JNK: c-Jun N-terminal kinase, ETC: electron transport chain

The illustration was taken from: "Drug-Induced Liver Injury: Clinical Evidence of N-Acetyl Cysteine Protective Effects" published by Ntamo, Ziqubu, Chellan, Nkambule, Nyambuya, Mazibuko-Mbeje, et al., in 2021 (89). Licensed under CC BY 4.0.

1.6.2. Cisplatin

Cis-diamminedichloroplatinum (CDDP), commonly referred to as cisplatin, is an anticancer agent used in a variety of cancers (90). Its chemical structure is depicted in **Figure 8**.

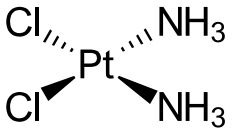

Figure 8: Chemical structure of cisplatin

Cisplatin uptake into the cell is mediated by membrane-bound transporters. Proteins that have been identified for this purpose include copper transporters such as CTR1, CTR2, and P-type copper transporting ATPases (91). In addition, organic cation transporters (OCTs) are also known to transport cisplatin across the cell membrane (91).

The mechanism of action of cisplatin involves oxidative stress with the formation of reactive oxygen species (ROS) and direct binding to DNA bases in its aquated form (90). The binding of cisplatin to DNA leads to monoadducts of cisplatin to the bases as well as to crosslinks within or between DNA strands that trigger DNA-repair or cell death (90). In addition, ROS are formed when cisplatin binds cytoplasmic molecules, such as glutathione and metallothionein (92). The resulting ROS further contribute to DNA damage and mitochondrial outer membrane permeabilization, leading to cell death (92). The mechanism of cisplatin toxicity is illustrated in **Figure 9**.

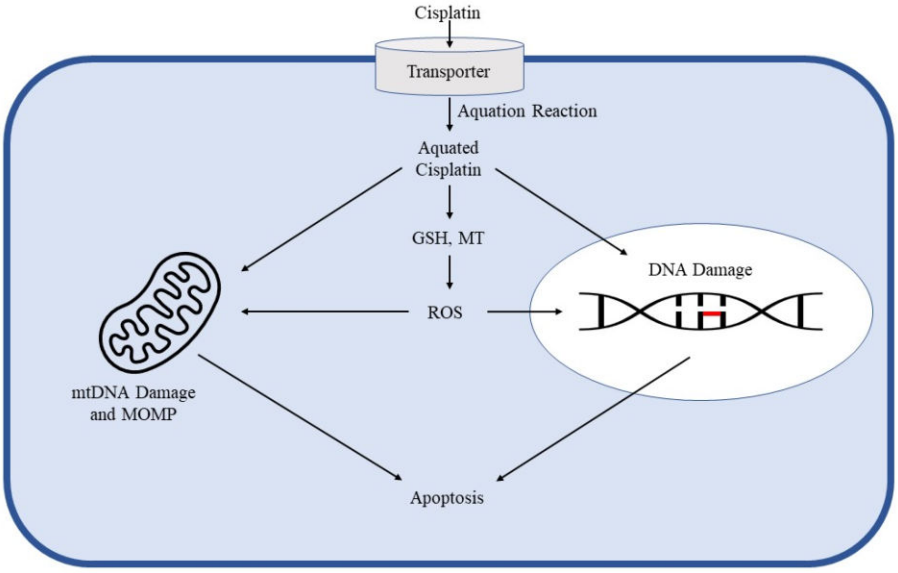

Figure 9: Mechanism of cisplatin cytotoxicity

Schematic illustration of cisplatin cytotoxicity. Cisplatin is aquated inside the cell after its diffusion through membrane transporters. The aquated cisplatin causes damage to nuclear and mitochondrial DNA and causes MOMP. When cisplatin is binding GSH and MT, ROS are formed. The ROS further contribute to DNA damage. DNA damage and MOMP result in apoptosis. mtDNA: mitochondrial DNA, MOMP: mitochondrial outer membrane permeabilization, GSH: glutathione, MT: metallothionein, ROS: reactive oxygen species.
The illustration was taken from: "Targeting DNA Damage Response and Repair to Enhance Therapeutic Index in Cisplatin-Based Cancer Treatment" published by Kiss, Xia and Acklin in 2021 (93). Licensed under CC BY 4.0.

This cytotoxicity does not confine itself to tumor cells. In fact, cisplatin has lots of toxic side effects on normal healthy cells in various organs. The drug-limiting toxicity of cisplatin is its severe nephrotoxicity (94). Although, hepatotoxicity is also a serious side effect. It is assumed that the hepatotoxic effects of cisplatin are primarily due to oxidative stress in the mitochondria and their subsequent dysfunction (94). It was also shown that cisplatin hepatotoxicity is exacerbated by higher CYP2E1 concentrations through an increase in ROS production (95). It is worthwhile noting that CYP2E1 in addition to its localization in the endoplasmic reticulum is also present in the mitochondria (96). In addition, DNA damage from ROS is generally more substantial in mitochondria than in nuclear DNA (97).

1.6.3. Isoniazid

Isoniazid, or isonicotinic acid hydrazide (INH), is an antituberculotic antibiotic. Its chemical structure is depicted in **Figure 10**.

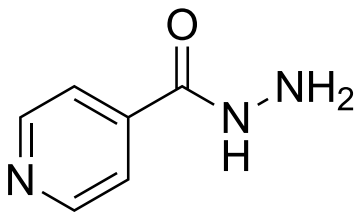

Figure 10: Chemical structure of isoniazid

Isoniazid is bactericidal to sensitive *Mycobacterium tuberculosis* strains (98). Isoniazid is activated by catalase peroxidase in the mycobacteria and subsequently binds nicotinamide adenine dinucleotide (NAD). INH-NAD inhibits the enoyl-acyl carrier protein reductase (InhA) halting mycolic acid synthesis (99).

In 1-3 % of patients, isoniazid causes a drug-induced liver injury (100). The mechanism of this reaction remains unclear (100). The idiosyncrasy of this liver injury has made it difficult to reproduce it in healthy animals (100). The metabolite hydrazine is thought to play a decisive role in its hepatotoxicity. Hydrazine depletes ATP in hepatocytes (101), inhibits mitochondrial complex II (102), and forms reactive electrophiles (103).

Isoniazid is also known to covalently bind to hepatic proteins (104). Therefore, the reason for the idiosyncrasy might be caused by an immune response. Patients with mild INH-induced liver-injury were reported to had an increase in T_H17-cells (105), while another study detected anti-INH and anti-cytochrome P450 antibodies in patients with INH-induced liver-injury (106). Yet, it is not clear if the antibodies cause the liver-injury (106).

1.6.4. Melatonin

Melatonin is a hormone of the pineal gland. The chemical structure of melatonin is depicted in **Figure 11**.

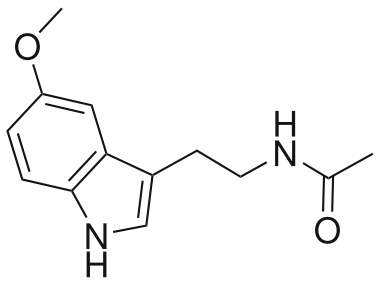

Figure 11: Chemical structure of melatonin

It is synthesized from serotonin and secreted according to the light-dark cycle (107). Its secretion is linked to the time spent in darkness (107). The hormone has lots of effects on bodily functions such as body temperature, cell regulation, and the immune system (107, 108). It has been thought of as a circadian synchronizer (107, 108). In addition to its circadian effects, melatonin is also an antioxidant able to neutralize ROS and RNS (109).

Melatonin has been reported to have numerous protective effects on the liver, including against drug-induced liver injury (110). Among others, it has been reported to be directly hepatoprotective in acetaminophen and cadmium-induced hepatotoxicity (111, 112) and to improve mitochondrial function (111). Therefore, no significant toxicity was expected with melatonin treatment, and it was chosen as a control substance in the treatment of PCLS in this thesis.

1.6.5. N-Acetylcysteine

N-Acetylcysteine (NAC) is an antioxidant thiol (113). The chemical structure is displayed in **Figure 12**.

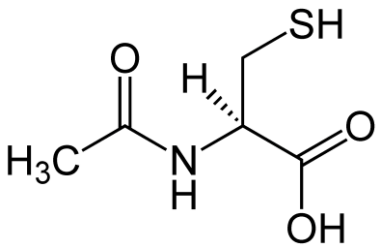

Figure 12: Chemical structure of N-Acetylcysteine

It is currently used clinically as a mucolytic and an antidot to acetaminophen poisoning (113). Mucolytic properties derive from the ability to break disulfides in glycoproteins (114). It counteracts acetaminophen toxicity by replenishing GSH, to eliminate the toxic NAPQI metabolite (113, 115).

NAC has a direct antioxidant effect on nitrogen dioxide (NO_2) and hypohalous acids such as hypochlorous acid (HOCl) (113, 116). Its antioxidant effect is indirectly enhanced by the fact that it is also a precursor of the endogenous antioxidant GSH and cleaves disulfides to enable the formation of new thiols (113, 116). This is why it was used as a sample- antioxidant on PCHS.

1.6.6. TEMPOL

4-Hydroxy-TEMPO (TEMPOL) is a derivative of the stabilized radical TEMPO, formally 2,2,6,6-tetramethylpiperidine-1-oxyl (117). Its chemical structure is depicted in **Figure 13**.

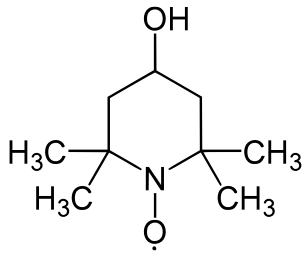

Figure 13: Chemical structure of TEMPOL

TEMPOL is an antioxidant. It can metabolize superoxide (O_2^-) to hydrogen peroxide (H_2O_2) as effective as the cellular superoxide dismutase (118). This is why it is often called a 'superoxide dismutase mimetic' (119). But TEMPOL can metabolize more than just superoxide. It is able to detoxify many different ROS, including H_2O_2, hydroxyl radicals ($^{\bullet}OH$) and peroxidation products (119). Which is why it was used as a sample-antioxidant on PCHS.

1.7. Objectives

The importance of research in the field of PCTS is obvious. While the Institute of Toxicology of the Heinrich-Heine-University already had an established model of precision-cut kidney slices, improvements in precision-cut liver and heart slices were lacking. This is why the thesis confined itself to PCTS of these two organs.

The incubation conditions of the PCTS should be characterized and improved before further toxicological research can be started. Optimal baseline viability of the slices is sought for. For this purpose, the effect of various factors will be examined with the help of viability assays. The PCLS can be tested for the impact of varying their slice thicknesses, as well as changes in the composition of the culture medium. The culture medium can be attempted to be improved by changing the glucose concentration, and by gassing it with carbogen (95% O_2, 5% CO_2). PCHS will be tested for the impact of varying the slice thickness, the usage of a cardioplegic solution during slicing, and the use of antioxidants during incubation. These factors are not only thought as possible improvements of the cutting and incubation process but will also reveal the sensitivity of PCTS to changes made in the protocol.

In addition, PCLS should be characterized histologically. Quantitatively, this can be evaluated with the nuclei number and nuclei area on the slices as well as their binucleated cells. PCLS will also be tested for protein expression of selected phase I and phase II biotransformation enzymes. This can reveal information about the functionality of the hepatocytes in the PCLS.

Following these tests, the PCLS will be treated with the model substances acetaminophen, cisplatin, isoniazid, and melatonin. The selected substances reflect different toxicologic profiles. Toxic reactions are expected with acetaminophen and cisplatin, as acetaminophen is a classic hepatotoxin and cisplatin is cytotoxic across cell types. In contrast, isoniazid induces toxicity only indirectly. While melatonin is used to demonstrate a non-toxic substance. The survival of the treated PCLS can be quantified with viability assays as well as histological analysis. The characterization of the reaction of PCLS to the selected test substances should provide information on their suitability for further toxicological investigations.

2. Materials and Methods

2.1. Materials

2.1.1. Chemicals, reagents, media

In the following, the used chemicals, reagents, and solutions are listed (**Table 1**).

Table 1: Used chemicals, reagents and solutions

Material	Manufacturer	Manufacturers' reference number or product name
0.5% Eosin	Carl Roth GmbH + Co. KG, Karlsruhe, Germany	X883.2
Acetaminophen	Sigma-Aldrich, St. Louis, MO, USA	A5000
Acetic acid	Carl Roth GmbH + Co. KG, Karlsruhe, Germany	6755.2
Agarose, low melting temperature	Sigma-Aldrich, St. Louis, MO, USA	A9414
Belzer UW® Cold Storage Solution	Bridge to Life (Europe) Ltd., London, UK	Belzer UW® Cold Storage Solution
Bovine serum albumin	Sigma-Aldrich, St. Louis, MO, USA	B6917
Cardioplegia solution	Dr. Franz Köhler Chemie GmbH, Bensheim Germany	Custodiol®
Cisplatin	Sigma-Aldrich, St. Louis, MO, USA	232120
D-(+)-Glucose solution	Sigma-Aldrich, St. Louis, MO, USA	G8644
D-Glucose	Sigma-Aldrich, St. Louis, MO, USA	G8270
EDTA	Sigma-Aldrich, St. Louis, MO, USA	E5134

Entellan™	Merck KGaA, Darmstadt, Germany	1.07961
Ethanol	VWR Chemicals, Radnor, PA, USA	20821
Formaldehyde 4.5%	Carl Roth GmbH + Co. KG, Karlsruhe, Germany	2213.1
Gentamicin	Gibco (Thermo-Fisher), Waltham, MA, USA	15750037
GlutaMAX™	Gibco (Thermo-Fisher), Waltham, MA, USA	35050-038
Glycerol	Carl Roth GmbH + Co. KG, Karlsruhe, Germany	3783.1
Hematoxylin	Sigma-Aldrich, St. Louis, MO, USA	H9627
HEPES Buffer Solution	Gibco (Thermo-Fisher), Waltham, MA, USA	15630-056
Hydrochloric acid	Carl Roth GmbH + Co. KG, Karlsruhe, Germany	K025.1
Incidin™ rapid	Ecolab Deutschland GmbH, Monheim am Rhein, Germany	3097420
Insulin-Transferrin-Selenium	Roche Holding, Basel, Switzerland	11074547001
Isoniazid	Merck KGaA, Darmstadt, Germany	I3377
Isopropyl alcohol	VWR Chemicals, Radnor, PA, USA	20842
Isotonic sodium chloride solution	Fresenius, Bad Homburg vor der Höhe, Germany	B306175
Ketamine	Zoetis, Parsippany-Troy Hills, NJ, USA	Ketaset 100 mg/ml
Krebs-Henseleit-Buffer Powder	Sigma-Aldrich, St. Louis, MO, USA	K3753
Magnesium sulfate heptahydrate	Merck KGaA, Darmstadt, Germany	1.05886

Medium 199	Gibco (Thermo-Fisher), Waltham, MA, USA	11150-059
Melatonin	Bachem Holding, Bubendorf, Switzerland	4008335
MTT	Sigma-Aldrich, St. Louis, MO, USA	M5655
N-Acetylcysteine	Sigma-Aldrich, St. Louis, MO, USA	A7250
Penicillin-Streptomycin	Sigma-Aldrich, St. Louis, MO, USA	P0781
Potassium alum	Merck KGaA, Darmstadt, Germany	1.01047
Potassium chloride	Sigma-Aldrich, St. Louis, MO, USA	P9333
Potassium dihydrogen phosphate	Merck KGaA, Darmstadt, Germany	1.04873
Potassium iodate	Sigma-Aldrich, St. Louis, MO, USA	215929
ROTI®-Histol	Carl Roth GmbH + Co. KG, Karlsruhe, Germany	6640.1
Sodium bicarbonate solution	Sigma-Aldrich, St. Louis, MO, USA	S8761
Sodium chloride	VWR Chemicals, Radnor, PA, USA	27810
Sodium hydroxide	Merck KGaA, Darmstadt, Germany	1.06498
Sterile-filtered water	Sigma-Aldrich, St. Louis, MO, USA	W3500
TEMPOL	Sigma-Aldrich, St. Louis, MO, USA	581500
Tris-HCl	Carl Roth GmbH + Co. KG, Karlsruhe, Germany	9090.3
Williams' Medium E	Sigma-Aldrich, St. Louis, MO, USA	W4128

Xylazine	Bayer, Leverkusen, Germany	Rompun® 2%

2.1.2. Equipment and consumables

Table 2 gives a detailed overview of the used laboratory equipment while sparing common household items, as microwaves, freezers, or fridges. And **Table 3** and **Table 4** list the used kits and laboratory consumables.

Table 2: Used equipment

Equipment	Manufacturer	Model
Centrifuge	Eppendorf SE, Hamburg, Germany	5415 R
Cooling plate (for specimens embedded in paraffin)	Leica Biosystems, Wetzlar, Germany	Leica EG1150 C
Heating plate (for histological slides)	C&A Scientific, Sterling, VA, USA	Premiere® XH-2001
Incubator	Binder GmbH, Tuttlingen, Germany	9040-0040
Krumdieck tissue slicer	Alabama Research & Development, Munford, AL, USA	MD6000
Laminar flow bench	Thermo-Fisher, Waltham, MA, USA	Hera safe KS 18
Microplate reader	Tecan Group AG, Männedorf, Switzerland	Infinite F200
Microplate reader	Tecan Group AG, Männedorf, Switzerland	Sunrise
Microscope	Leica Biosystems, Wetzlar, Germany	Leica DM750
Microtome	Carl Zeiss AG, Oberkochen, Germany	Hyrax M 25
Oven	Memmert GmbH + Co. KG, Schwabach, Germany	SLM 400

Paraffin casting machine	Leica Biosystems, Wetzlar, Germany	Leica EG1150 H
Pipettes	Eppendorf SE, Hamburg, Germany	Research® plus
Shaker (in viability assays)	Edmund Bühler GmbH, Bodelshausen, Germany	KL-2
Shaker (in the incubator)	Grant Instruments (Cambridge) Ltd., Royston, UK	PMR-30
Sonicator	Active Motif Inc., Carlsbad, CA, USA	EpiShear™
Spectrophotometer	General Electric Company, Boston, MA, USA	NanoVue™ Plus
Thermocycler	Biometra GmbH, Göttingen, Germany	T-personal-thermocycler
Tissue Lyser	Qiagen, Hilden Germany	TissueLyser II
Water bath (for stretching paraffin slides)	GFL Technology, Lauda-Königshofen Germany	GFL 1052
Water distiller	Merck KGaA, Darmstadt, Germany	Milli-Q

Table 3: Used kits

Kit	**Manufacturer**
ATPlite Luminescence Assay System Kit	PerkinElmer, Waltham, MA, USA
DCTM protein assay	Bio-Rad Laboratories, Inc., Hercules, CA, USA
High-Capacity cDNA Reverse Transcription Kit	Thermo-Fisher, Waltham, MA, USA
PowerTrack SYBR Green Master Mix	Thermo-Fisher, Waltham, MA, USA

RNeasy® Mini QIAcube-kit	Qiagen, Hilden, Germany

Table 4: Used consumables

Consumable	Manufacturer
12-well-plates	Sarstedt AG & Co. KG, Nümbrecht, Germany
96-well-plates (for MTT assay)	Greiner Bio-One, Kremsmünster, Austria
Adhesive specimen slides	Epredia, Portsmouth, NH, USA
Conical tubes	Greiner Bio-One, Kremsmünster, Austria
Micro test tubes	Eppendorf SE, Hamburg, Germany
Opaque 96-well plates (for ATP assay)	Nunc™ (Thermo-Fisher), Waltham, MA, USA,
Parafilm®	witeg Labortechnik GmbH, Wertheim, Germany
Petri dishes	Greiner Bio-One, Kremsmünster, Austria
Pipette tips	TipOne®, Starlab GmbH, Hamburg, Germany
Syringes	B. Braun Melsungen AG, Melsungen, Germany
Tissue cassettes	Carl Roth GmbH + Co. KG, Karlsruhe, Germany

2.1.3. Oligonucleotide primers

In the following, **Table 5** lists the oligonucleotide primers used and their sequences.

Table 5: Used oligonucleotides and their sequences

Name	Forward sequence	Reverse sequence
Cyp1a1	GGTAGTTCTTGGAGCTTCCCC	ATGATCTAGGTGGCTGCTTGG
Cyp2c29	CCCCATGGTTGCAGGTAAAC	ACCACACGGTCAATCTCTTCC
Cyp2e1	CTCAAAAAGACCAAAGGCCAGC	CCAGGGAGTACTCAGCAGGT
Cyp3a11	CCTGGGTGCTCCTAGCAATC	ACCATCAAACAACCCCCATGT
Gapdh	TCTCCTGCGACTTCAACA	TCTCTTGCTCAGTGTCCTT
Gstα3	GCAGCTGGTGTGGAGTTTGA	GCCAGGTCATCCCGAGTTTT
Sult1c2	CCGGCGAACCATCATTCAAC	AGCTGGCATCTCATTGGCTT
Ugt-1	TGGCTGACTGGAAACCGAC	GAAGGCAAGCCATCCTGTCA
β-actin	CCTGTATGCCTCTGGTCGTA	CCATCTCCTGCTCGAAGTCT

2.1.4. Animals

Wild-type male C57BL/6J mice were used for the experiments. The mice had an age of over 14 weeks and were obtained from the Central Institution for Animal Research and Scientific Animal Welfare (ZETT) of the Heinrich-Heine-University or the Janvier Labs (Le-Genest-Saint-Isle, France).

The organ removal of the mice was authorized by the ZETT under the authorization number O55/16. The handling and sacrifice of the animals was done in accordance with the German animal welfare act. For this purpose, Ahmed Emre Erbay received education from the ZETT on April 25th, 2022.

2.1.5. Software

Analysis of data was performed with Microsoft Excel and GraphPad Prism 6.01 (GraphPad Software, Inc.). Furthermore, GraphPad Prism 6.01 was used to design graphs to display the data. Images were analyzed with Fiji 2.9.0.

2.2. Generation of precision-cut tissue slices

This methodology follows the approach described in our preprint (1).

2.2.1. Preparations before organ removal

Before organs could be removed from the animals, several preparations were made. First, the different culture media required for PCLS and PCHS incubation were freshly prepared on the day of organ removal under the laminar flow clean bench. The finished medium was then put in a 37 °C water bath to keep it warm. The composition of the culture medium is further explained in chapter 2.3.1.

All components of the Krumdieck tissue slicer were sterilized with 80 % ethanol and put together according to the manufacturer's instructions. 2 % LMP-Agarose, composed of 400 mg LMP-agarose in 20 mL PBS, was boiled up in the microwave and put into the oven at 40 °C to cool down. Belzer UW® Cold Storage solution was filled into conical tubes and kept on ice.

Krebs-Henseleit-Buffer (KHB) was prepared one day before organ removal. It was prepared by adding solutions to a pre-prepared salt mixture according to **Table 6**. Initially, a premanufactured mixture was used. While later, the mixture was self-prepared according to **Table 7**. After preparation of the KHB the pH was set to 7.2 with 1 M HCl. On the day of organ removal, the KHB was kept at -20 °C for 30 minutes.

Table 6: Preparation of Krebs-Henseleit-Buffer

Material	Volume
Krebs-Henseleit Buffer (powder)	powder already prepared for 1L water
Water, sterile-filtered	1 L
HEPES buffer solution (1 M)	10 mL
D-Glucose solution (100 g/L)	25 mL
$NaHCO_3$ solution (7.5 %)	28 mL

Table 7: Composition of Krebs-Henseleit-Buffer salt mixture

Chemical	Weight
D-Glucose	2000 mg
$MgSO_4*7H_2O$	289 mg
KH_2PO_4	160 mg
KCl	350 mg
NaCl	6900 mg

When the effects of carbogen gassing were examined, the KHB was additionally gassed 30 minutes with carbogen immediately before organ removal at the Institute for Experimental Nephrology.

2.2.2. Organ removal

Before organ removal could take place, the mice were killed by cervical dislocation under anesthesia. The mice were anesthetized with 8 mg xylazine and 120 mg ketamine per kg body weight. A xylazine-ketamine solution was prepared, in which 0.8 mL of isotonic NaCl solution was mixed with 0.1 mL of 2 % xylazine and 0.3 mL of 10 % ketamine. The mouse was weighed, and the appropriate amount of xylazine-ketamine solution was injected i.m. according to **Table 8**:

Table 8: Injected anesthesia dose according to the weight of the mice

Weight	20 g	25 g	30 g	35 g	40 g	45 g
Volume	0.08 mL	0.10 mL	0.12 mL	0.14 mL	0.16 mL	0.18 mL

The liver and heart of the wild-type C57BL/6J mice were removed by Ronja Brinks, Frauke Roolfs or Ahmed Emre Erbay and were placed in conical tubes with Belzer UW® Cold Storage solution. The tubes were kept on ice. When the effect of a cardioplegic solution on PCHS was examined, the heart was placed in a conical tube with Custodiol®.

2.2.3. Production of precision-cut tissue slices

Ice-cold KHB was filled into the Krumdieck tissue slicer in which the organs were ultimately cut. When the effect of a cardioplegic solution on PCHS was examined, the heart was cut in cold Custodiol®. For better visualization, a picture of the Krumdieck tissue slicer is depicted in **Figure 14**.

Figure 14: Set up of the Krumdieck tissue slicer

A: oscillating arm that moves the holding apparatus back and forth. B: cylindrical holding apparatus containing the organ, beneath the holding apparatus is a razor blade located. C: basin containing the holding apparatus, filled with KHB or Custodiol® during operation. D: controller of the slice thickness. E: catch basin for the PCTS, which can be drained into a bottle after the organ is cut.

The two organs were placed differently into the slicer before operation. The liver was punched out in a diameter of approximately 8.5 cm which is depicted in **Figure 15** and placed in 2 % LMP-Agarose in the tissue holding apparatus of the machine. For this 3 - 5 drops of 2 % LMP-Agarose were pipetted first. Afterwards, the punched-out liver piece was placed into the apparatus and 3 - 5 drops of 2 % LMP-Agarose were pipetted again on top of the liver. While the heart was embedded in 2 % LMP-Agarose in the holding apparatus, as a whole. After 30 seconds to 1 minute the 2 % LMP-Agarose congealed and was ready to be cut.

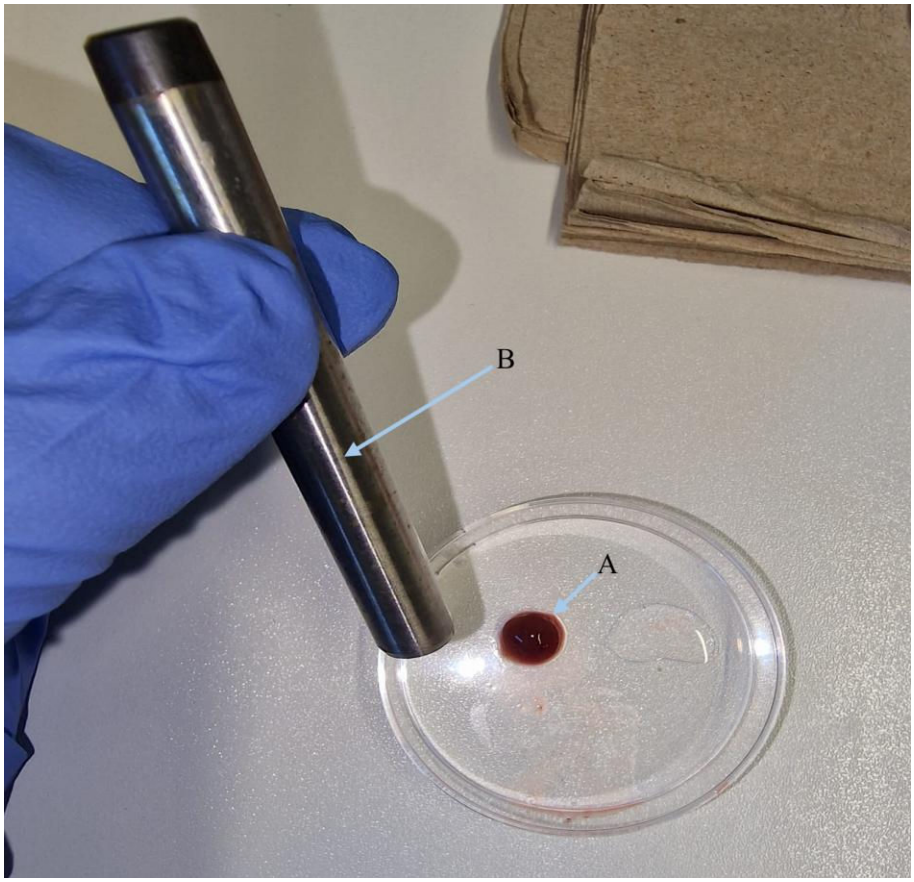

Figure 15: Punched-out liver

A: punched-out liver piece B: punching equipment of the tissue slicer

The slice thickness was manually adjusted to 200 µm, 250 µm or 300 µm respectively, before the cutting process. After starting the machine, the holding apparatus moved back and forth a sharp razor blade by the tissue slicer. The forming tissue slices were then collected into a 2 L laboratory bottle. The tissue slices were then immediately transferred to a new conical tube with Belzer UW® Cold Storage solution or Custodiol® on ice.

2.3. Culture of precision-cut tissue slices

This methodology follows the approach described in our preprint (1).

2.3.1. Culture media

The basic composition of the medium used for cultivating the PCLS was freshly prepared according to **Table 9**:

Table 9: Composition of PCLS culture medium

Material	Volume
Williams' Medium E	40 mL
GlutaMAX™ (200 mM)	400 µL
Gentamicin (50 mg/ml)	40 µL

Additionally, further adjustments were made to this medium composition when specific effects of added compounds were examined. The adjustments that were made are listed in **Table 10**:

Table 10: Compounds added to the PCLS medium

Added compound	Reference to chapter
100 g/L D-Glucose	3.1.2
20 mM Acetaminophen	3.4.1
1 g/L Cisplatin	3.4.2
20 mM Isoniazid	3.4.3
0.2 g/L Melatonin	3.4.4

When the effect of carbogen gassing on the PCLS was tested, the medium was additionally gassed with carbogen for 15 minutes immediately before organ removal at the Institute for Experimental Nephrology.

A different medium was used for the PCHS. The composition is described in **Table 11**. The adjustments that were made to the PCHS medium are listed in **Table 12**.

Table 11: Composition of PCHS culture medium

Material	Volume
Medium 199	25 mL
Penicillin/Streptomycin	250 µL
Insulin-Transferrin-Selenium (10mg/ml)	25 µL

Table 12: Compounds added to the PCHS medium

Added compound	Reference to chapter
5 mM N-Acetylcysteine	3.1.6
5 mM TEMPOL	3.1.6

All added compounds were self-prepared except for 100 g/L D-Glucose solution (obtained by Sigma-Aldrich). For this purpose, the drugs were dissolved in the stated concentration in distilled water. The compounds were then diluted to the desired concentrations in the medium of PCLS and PCHS.

2.3.2. Incubation

After the cutting process was complete, the PCLS and PCHS were transferred to a petri dish under the laminar flow clean bench together with their storage solution.

A prelabeled 12-well plate was filled with 1 mL of medium per well and the PCTS were then transferred to their respective well by spatula. The 12-well plate was then incubated on a shaker at 37 °C with 21 % O_2 and 5 % CO_2. The moment in which the slices were put into the incubator was set as zero. If a slice was incubated for 48 hours, its medium was changed after 24 hours after the incubation started.

2.3.3. Sterile work

Efforts were made to keep the organs and their PCLS and PCHS in as sterile environments as possible. The Krumdieck tissue slicer was sterilized with 80 % ethanol before use. After the cutting process, the tissue slicer was washed thoroughly with water. The sterile laminar flow clean bench was sterilized with Incidin™ rapid before and after its use. Additionally, every item was sterilized with 80 % ethanol before being put under the laminar flow clean bench, as were the gloved hands. While working under the laminar flow clean bench, aseptic techniques were used. Fluids and disposables used

under the laminar flow clean bench were autoclaved if not already sterile and glass items were heat sterilized.

Unfortunately, though, sterility was not possible to maintain in some circumstances. Although the tissue slicer was sterilized with ethanol to reduce contamination, the machine could not be operated in a fully sterile manner. Additionally, the gassing of culture medium and KHB with carbogen could not be operated fully sterile either.

2.4. Viability assays

Viability assays were used to quantify the metabolic activity of the PCTS over time. The effects of changes to the incubation protocol or the effects of PCTS treatment were measured via changes in metabolic activity. For this purpose, the following established assays were used. These viability assays were also described in our preprint (1).

2.4.1. MTT assay

The 3-(4,5-dimethylthiazol-2-yl)-2,5-diphenyltetrazolium bromide (MTT) assay, established by *Mosmann* in 1983, is a colorimetric assay used to assess the viability of cells (120). MTT is a tetrazolium dye that is formed into insoluble formazan in active mitochondria (120). The reaction is depicted in **Figure 16**.

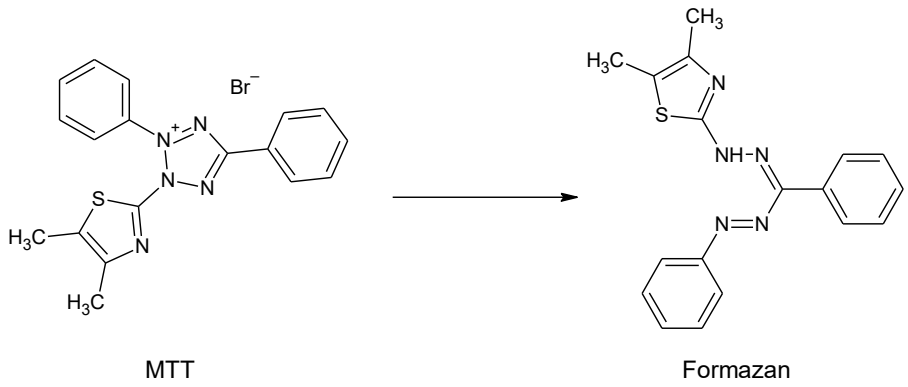

Figure 16: Chemical reaction of MTT to Formazan

The formazan can then be solubilized by a solvent, such as dimethyl sulfoxide or isopropyl alcohol (121, 122). The optical density can then be used as a measure of formazan's concentration in the solvent and thereby the viability of the tested cells (121). The assay is known to display linearity up to 10^6 cells in cell cultures (121). It was also already used on PCLS cultures previously (123, 124). In principle though, the assay measures the metabolic activity of the cells which is seen as a marker for their viability (125). This is why the term 'metabolic activity' was later used in this thesis to describe the results.

To perform the MTT assay 260 µL of 3.5 mg/ml MTT dissolved in water was added to the medium in each well of the 12-well plate. After that, the plate was incubated for 1 hour at the same conditions as previously, at 37°C with 21 % O_2 and 5 % CO_2.

After the incubation period, the PCLS and PCHS were weighed and transferred to a new 12-well plate. Each well was then filled with 1 mL of isopropyl alcohol. The 12-well plate was then sealed with Parafilm® and wrapped in aluminum foil and shaken on a shaker for 30 minutes.

From the dyed isopropyl alcohol of each well, 100 µL was pipetted into 4 wells of a 96-well plate. The optical density was then measured at 560 nm on a microplate reader (Sunrise, Tecan Group AG). Isopropyl alcohol was used as a control. The mean optical density of each sample minus the optical density of the control was then related to the weight of the tissue slice. Either the mean metabolic activity of PCTS at 0 h of incubation or the mean metabolic activity of the untreated PCTS was set as 100 % viability, depending on the experiment.

2.4.2. ATP assay

Another option to quantify the viability of the PCTS is via adenosine triphosphate (ATP). ATP is the primary energy carrier of cells. The cleavage of phosphate groups offers the energy needed for biochemical reactions (126). Cell death first halts new ATP synthesis (126). Therefore, it can be seen as the main indicator to measure viability (126). ATP has also been used to assess the viability of PCLS in prior studies (38, 39, 41). As ATP production is closely linked to the metabolic activity of the cell, the term was also used in the description of the results in this thesis.

The assay that was used to measure the ATP content was based on the luciferinase-catalyzed oxidation of D-luciferin in the presence of ATP, producing oxyluciferin and light. The emitted luminescence is proportional to the ATP concentration and can be measured with a luminometer (127). The reaction is depicted in **Figure 17**.

Figure 17: Chemical reaction of Luciferin to Oxyluciferin

To prepare the PCTS for the adenosine triphosphate (ATP) viability assay, the PCTS were transferred to a prelabeled 2 mL micro test tube containing 500 µL of solution A and were shock-frozen using liquid nitrogen. Thereafter the micro test tube was stored at -80 °C. The ATP viability assay could then be performed at any time.

Before the ATP viability assay was started, conical tubes containing 4.5 mL of solution B were prepared on ice. The composition of solutions A and B is listed in **Table 13**.

Table 13: Solutions used in the ATP assay

Solution	Composition
Solution A	100 mL 70 % Ethanol 0.058 g EDTA pH: 10.9
Solution B	100 mL H_2O 1.56 g Tris-HCl 0.058 g EDTA pH: 7.9

After the frozen micro test tubes thawed on ice, one metal ball of 8 mm diameter and one metal ball of 5 mm diameter was added to the micro test tube. The PCTS were then lysed 3 times for 30 seconds at 30 Hz using the TissueLyserII (Qiagen). The components of the tissue lyser were stored at 4 °C before use. The metal balls were then removed, and the tubes were centrifuged at 16000 G at 4 °C for 2 minutes. The formed supernatant was then pipetted into the prepared conical tubes containing 4.5 mL of solution B. This mixture of solution B and the supernatant of the lysed PCTS was subsequently used for the ATP detection. The remaining pellet that formed after centrifugation was used for protein determination.

For ATP detection 100 µL of the probe was pipetted from the conical tubes into a white opaque 96-well plate, using triplets. Then 50 µL of substrate from the ATPlite Luminescence Assay System Kit (PerkinElmer) was added to each well as instructed by the manufacturer. The 96-well plate was shaken for 5 minutes and afterwards kept dark for 10 minutes. At the end the luminescence was measured on a microplate reader (Infinite F200, Tecan Group AG).

The ATP molar concentration was calculated using a standard dilution series. The standard dilution was prepared in solution B using the 100 µM ATP standard stock of the kit. The ATP molar concentration was then related to the protein concentration, which was obtained from the protein determination of the pellet that was formed after centrifugation. The protein determination could be started in parallel to the ATP detection or delayed to a later point in time while the probes were stored at -80 °C.

For the protein determination, 200 µL of 5 M NaOH was added to the micro test tube with the pellet on ice and it was waited for 30 minutes. Then 800 µL of H_2O were added to dilute the NaOH. The probe was repetitively pipetted to dissolve the pellet and its proteins. Afterwards, the samples were treated with the sonicator at 35% amplitude 5 times for 2 seconds. The protein determination was performed with the DCTM protein assay (Bio-Rad) according to the manufacturer's instructions and read out via a microplate reader (Sunrise, Tecan Group AG). The protein concentration was calculated using a standard dilution series of BSA in water.

The ATP molar concentration was then related to the protein concentration to get a relative ATP concentration. Either the mean relative ATP concentration at 0 h of incubation or the mean relative ATP concentration of the untreated PCTS was set as 100 % viability, depending on the experiment.

2.5. Histology

The methodology described here follows the approach we described in our preprint (1). To prepare the PCTS to be used in histology, the sample must be fixated first. This is commonly done with formaldehyde (128). Methylene glycol, the hydrate of formaldehyde, slowly reacts chemically with the tissue, thereby fixating it (128). Next, the free water of the samples is displaced by alcohol (128). The sample is then embedded and infiltrated by paraffin, which allows it to be cut on a microtome and stored (128). Before the final staining, slices have to be deparaffinized again (128).

In our protocol, the PCTS were transferred to a micro test tube containing 4.5 % formaldehyde by spatula and kept overnight. The next day, they were transferred to tissue cassettes and submerged in PBS and kept at 4 °C. The PCTS were then dehydrated at the Institute for Pharmacology by machine. The dehydrated slices were embedded in paraffin and cooled down to harden. Afterwards, they were cut at 3 µm with a microtome and transferred onto warm water in a water bath, to let the paraffin

stretch. Thereafter, they were transferred onto an adhesive specimen slide and dried on a heating plate.

2.5.1. Hematoxylin and eosin staining

Hematoxylin and eosin staining is a standard histological procedure. Hematoxylin stains basophilic components of cells blue such as the nucleus, ribosomes, and rough endoplasmic reticulum (129). While eosin stains acidophilic, commonly called eosinophilic, components of the cell pink such as the cell membrane, lysosomes, mitochondria, smooth endoplasmic reticulum, microtubules, and proteins (129). Lipid vacuoles cannot be stained and appear empty (129).

In our protocol, the specimen slides were kept at 60 °C for 1 hour or at 37 °C over night. Afterwards the slides underwent deparaffinization according to the protocol depicted in **Table 14**:

Table 14: Deparaffinization protocol

3 cuvettes à 4 min	ROTI®-Histol
2 cuvettes à 3 min	100 % Ethanol
2 cuvettes à 3 min	96 % Ethanol
2 cuvettes à 3 min	70 % Ethanol
1 cuvette 1 min	distilled water

After deparaffinization the slides were stained in hematoxylin for 5 minutes. The hematoxylin was self-prepared prior to the staining and stored dark at room temperature. 2 g hematoxylin were dissolved in 99,8 % isopropyl alcohol. One by one 103.8 mL distilled water, 3 g potassium alum, 100 mL glycerol, 10 mL acetic acid, 0.4 g potassium iodate were added.

Bluing of hematoxylin was done for 15 minutes with tap water. Afterwards the slides were dyed in 0.5 % Eosin (with 2 drops added acetic acid) for 3 minutes. The slices were then dehydrated in an ascending alcohol series according to **Table 15**. Afterwards the slides were mounted with Entellan™.

Table 15: Ascending alcohol series

2 cuvettes à 4 dips	70% Ethanol
2 cuvettes à 6 dips	96% Ethanol
2 cuvettes à 3 min	100% Ethanol
3 cuvettes à 3 min	ROTI®-Histol

Photographs of the slides were made with a Leica DM750 microscope under 200x magnification and analyzed in Fiji 2.9.0.

2.6. PCR

2.6.1. RNA isolation

The RNA was isolated from the lysate of tissue samples, after lysing the tissue for 60 seconds in the TissueLyserII (Qiagen) at 30 Hz. The RNA isolation was done manually with the RNeasy® Mini QIAcube-kit (Qiagen) according to the manufacturer's instructions.

2.6.2. cDNA synthesis

Before the RNA could be used for the RT-qPCR it had to be transcribed into cDNA.
The RNA concentration was measured with the NanoVue™ Plus Spectrophotometer. Mixture A was prepared from the High-Capacity cDNA Reverse Transcription Kit (Thermo Fisher) on ice according to **Table 16**.

Table 16: Composition of Mixture A used in cDNA synthesis

Mixture A	**Amount per probe**
10x Buffer RT	2 µL
25x dNTP Mix [100 mM]	0.8 µL
10x random primers	2 µL
Riboblock RNase inhibitor [40 U/µL]	0.5 µL
Reverse Transcriptase	1 µL

The RNA probes were then thawed on ice. The needed volume of RNA (V_{RNA}) and RNase-free water ($V_{RNase\ free\ water}$) was calculated according to following equation:

$$V_{RNA} = \frac{2000\ ng}{[RNA]}$$

$$V_{RNase\ free\ water} = 13.7\ \mu L - V_{RNA}$$

RNA, RNase free water and Mixture A were then mixed and underwent the protocol depicted in **Table 17** in the thermocycler.

Table 17: cDNA synthesis thermocycling protocol

Temperature in °C	Duration in min
25	10
37	120
85	5
8	Infinite

The resulting cDNA was stored at -20°C until used in the RT-qPCR.

2.6.3. RT-qPCR

The RT-qPCR was prepared with 20 µL per well on a 96-well plate on ice with the substances listed in **Table 18** per well. Each cDNA was paired with each primer pair.

Table 18: Composition per well in RT-qPCR

cDNA	20 ng
SensiMix™ SYBR® Hi-ROX	1x
Forward Primer	0.25 µM
Reverse Primer	0.25 µM

The 96-well plate was sealed off and centrifuged. Afterwards it underwent the protocol listed in **Table 19** in the PCR cycler:

Table 19: PCR cycle

	Temperature	Duration
	95 °C	10 min
Cycle (45x):	95 °C	15 sec
	55 °C	15 sec
	72 °C	17 sec
	95 °C	1 min
	55 °C	1 min
	65 °C to 95 °C	1°C increase every 5 sec

The results were normalized to Gapdh and β-actin expression. Afterwards, the relative expression of the genes at 4 h of incubation was normalized to their expression at 0 h.

2.7. Statistics

The statistical analyses were performed with GraphPad Prism 6.01 (GraphPad Software, Inc.). Single values were compared to their respective control value with a two-tailed unpaired t-test. Multiple values (slice thicknesses of 200 µm, 250 µm and 300 µm in PCLS) were compared with a One-way ANOVA and a Tukey's multiple comparison test. The results were considered as statistically significant at values of $p \leq 0.05$.

3. Results

Parts of this chapter include data previously published in our preprint (1)

3.1. Effect of incubation conditions on metabolic activity

Prior to further assessment of the PCLS and PCHS, the effect of selected incubation conditions was tested. Variations in metabolic activity resulting from different incubation conditions had to be ruled out first, to assess the PCTS's sensitivity to mistakes in their handling and to establish optimal baseline conditions.

3.1.1. PCLS – effect of slice thickness

First, the metabolic activity of PCLS with different thicknesses was measured. For this purpose, the slice thicknesses of 200 µm, 250 µm, and 300 µm were selected. The metabolic activity was measured with the ATP and MTT assays over the course of 48 hours. The results are depicted in **Figure 18**. Parts of this figure were published (1).

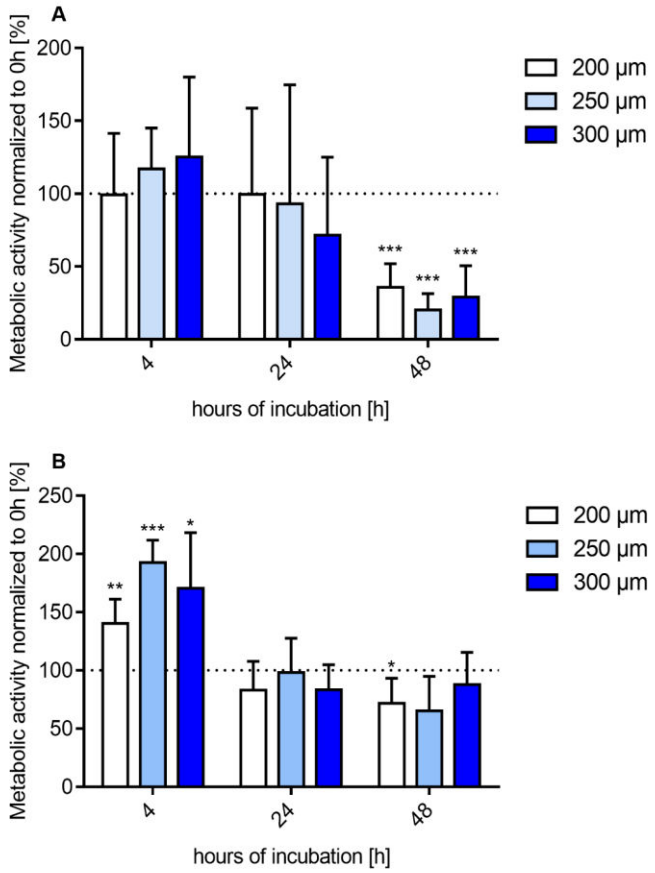

Figure 18: Effect of different slice thicknesses on the metabolic activity of PCLS

PCLS were cut to a thickness of 200 µm, 250 µm, and 300 µm and incubated for 4 h, 24 h, and 48 h, respectively. After the incubation period, the metabolic activity of the slices was assessed via ATP assay (A) and MTT assay (B) and normalized to a control taken before incubation. Depicted as mean + SD, n=4, N=1. (*: $p \leq 0.05$, **: $p < 0.01$, ***: $p < 0.001$, statistical significance vs. before incubation, unpaired t-test)

After 4 h of incubation, the PCLS demonstrated a metabolic activity close to conditions before incubation when assessed on ATP. While the MTT assay indicated a significant increase in metabolic activity throughout all slice thicknesses.

After 24 h of incubation, neither assay depicted significant increases nor decreases in metabolic activity from baseline activity. After 48 h of incubation though, a significant decrease in metabolic activity was observed throughout all slice thicknesses when assessed for ATP. This significant decrease was also demonstrated by 200 µm thick PCLS in the MTT assay. Yet, the thicker PCLS only showed a tendency of decreased activity.

A significant difference in metabolic activity between the different thickness groups was not detected at any period.

3.1.2. PCLS – effect of medium glucose concentration

Next, two different glucose concentrations in the culture medium were compared. One medium contained supra-physiologic glucose concentrations (25 mM), while the other contained 11 mM glucose, which is closer to the physiological intrahepatic glucose concentration (130). Again, the PCLS were evaluated regarding their metabolic activity over the course of 48 hours. In this stage of experiments, both 200 µm and 250 µm thick PCLS were included. The results are depicted in **Figure 19**. Parts of this figure have been published previously (1).

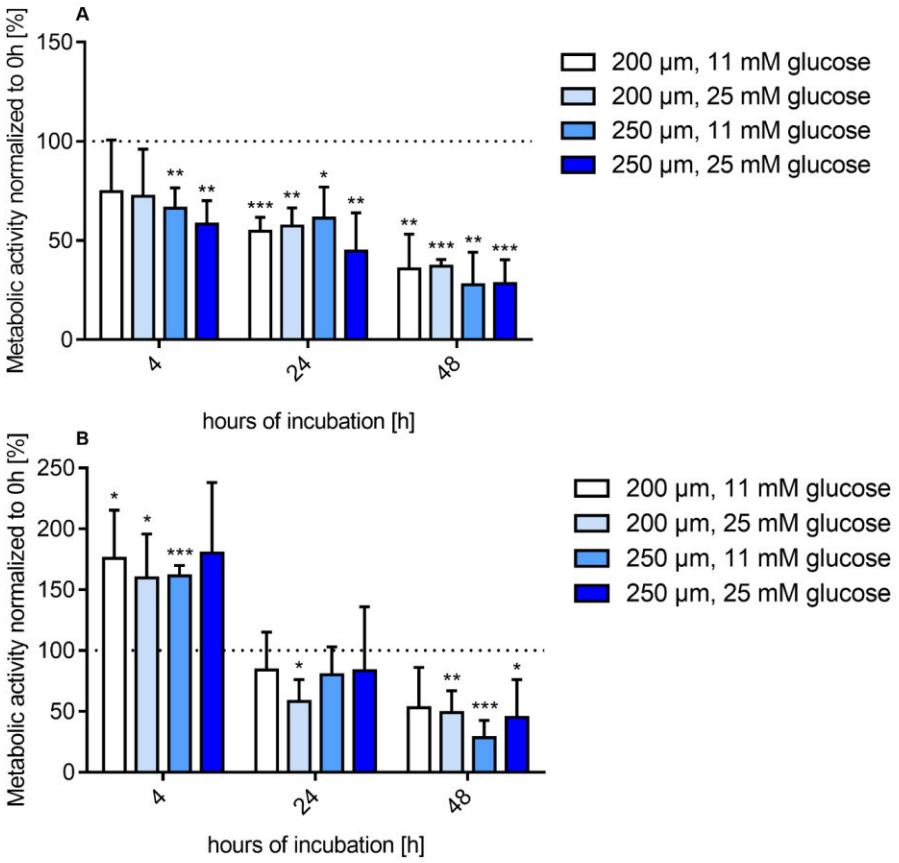

Figure 19: Effect of different glucose concentrations on the metabolic activity of PCLS

PCLS with a thickness of 200 µm and 250 µm were incubated for 4 h, 24 h, and 48 h in 11 mM or 25 mM glucose-containing medium, respectively. After the incubation period, the metabolic activity of the slices was assessed via ATP assay (A) and MTT assay (B) and normalized to the control before incubation. Depicted as mean + SD, n=3, N=3. (*: $p \leq 0.05$, **: $p < 0.01$, ***: $p < 0.001$, statistical significance vs. before incubation, unpaired t-test)

After 4 h of incubation, the metabolic activity was significantly decreased in 250 µm thick PCLS when assessed via the ATP assay, while the 200 µm thick PCLS only had a tendency of decreased activity. This stood in contrast to the measurements of the prior evaluation. On the other hand, almost all PCLS exhibited an increased metabolic activity after 4 h of incubation when assessed via the MTT assay. This result was compatible with the prior experiment.

After 24 h of incubation, all experimental groups had a significant decrease in metabolic activity when assessed via ATP assay. The assessment via MTT assay also showed a decrease in activity in all groups, which was only statistically significant in 200 µm thick PCLS in a high-glucose medium.

After 48 h of incubation, all experimental groups had a significant decrease in metabolic activity when assessed via ATP assay. This was also the case in all of the PCLS except 200 µm thick PCLS in low-glucose containing medium when assessed via MTT assay.

But overall, neither 200 µm thick PCLS nor 250 µm thick PCLS were significantly different from one another in terms of their metabolic activity. There were also no significant differences in activity, between the PCLS regarding the two glucose concentrations of their media. So, in further experiments, it was settled on using 250 µm thick PCLS, incubated in a medium containing 11 mM glucose.

3.1.3. PCLS – effect of carbogen gassing

It has been suggested that carbogen (95 % O_2, 5 % CO_2) could improve cell survival in PCLS due to a higher oxygen supply to the tissue. Therefore, the KHB in which the organs were sliced and the medium in which the PCLS were incubated was gassed with carbogen. The metabolic activity of PCLS that were incubated in carbogen-gassed culture medium and PCLS that were incubated under standard conditions was compared over the course of 48 hours and is depicted in **Figure 20**.

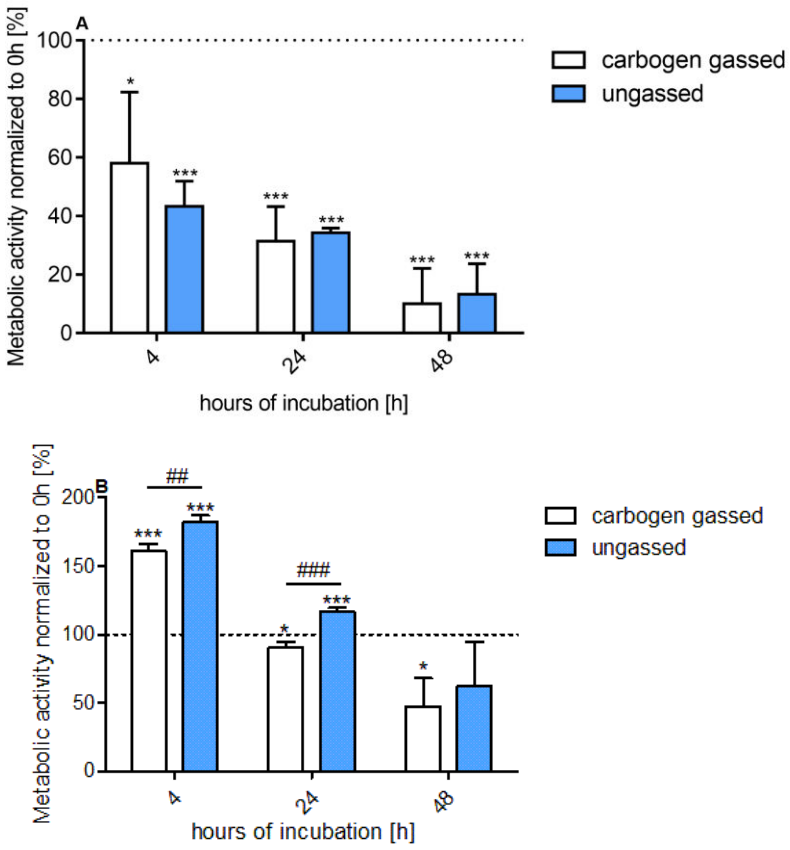

Figure 20: Effect of carbogen gassing on the metabolic activity of PCLS

Prior to incubation, the KHB in which the PCLS were sliced and the medium in which they were incubated was gassed with carbogen or remained ungassed. The PCLS were incubated for 4 h, 24 h, and 48 h. After incubation, the metabolic activity of the slices was assessed via ATP assay (A) and MTT assay (B) and normalized to the control before incubation. Depicted as mean + SD, n=3, N=3. (*: $p \leq 0.05$, ***: $p < 0.001$, ##: $p < 0.01$, ###: $p < 0.001$, asterisks depict statistical significance vs. before incubation, pounds depict statistical significance between two groups, unpaired t-test)

Parts of Figure 20 have been previously published (1).

While the ATP assay showed significant decreases in metabolic activity in all PCLS starting at 4 h of incubation, the MTT assay depicted a significant increase in activity after 4 h of incubation. This mirrored the prior experiments.

When measured with the MTT assay, the metabolic activity after 24 h of incubation was significantly increased in ungassed PCLS, while it was significantly decreased in gassed PCLS. After 48 h of incubation, a loss in metabolic activity was observed in all PCLS. This decrease was shown to be significant in gassed PCLS.
Regarding the differences between the gassed and ungassed slices, the ungassed slices had a significantly higher metabolic activity after 4 h and 24 h of incubation compared to gassed slices when assessed in the MTT assay, while the assessment with the ATP assay did not mark any significant differences between the two experimental groups.

3.1.4. PCHS – effect of slice thickness

The metabolic activity of 200 µm thick PCHS were compared to that of 250 µm thick PCHS (**Figure 21**).

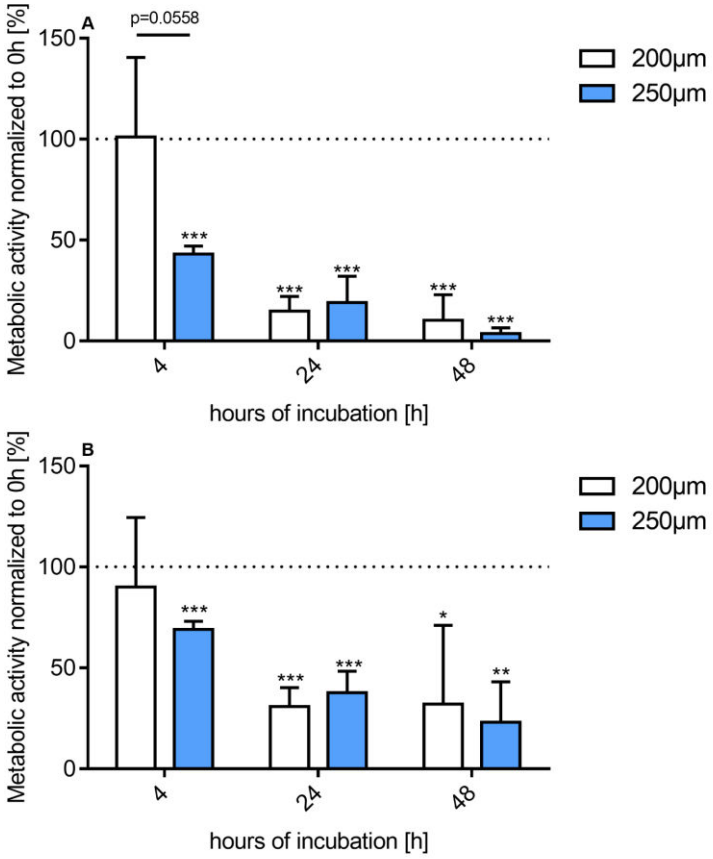

Figure 21: Effect of slice thickness on the metabolic activity of PCHS

PCHS were cut to a thickness of 200 µm or 250 µm and incubated for 4 h, 24 h and 48 h (n=4, N=1 for 200 µm and n=3, N=3 for 250 µm). They were assessed for their metabolic activity via ATP assay (A) and MTT assay (B). All values were normalized to the respective controls before incubation. Depicted as mean + SD. (*: $p \leq 0.05$, **: $p < 0.01$, ***: $p < 0.001$, statistical significance vs. before incubation, unpaired t-test)

After 4 h of incubation 250 µm thick PCHS were already significantly less metabolically active than PCHS before incubation. This was confirmed in both ATP and MTT assays. 200 µm thick PCHS had lower losses in activity. After 24 h and 48 h of incubation, the activity of all PCHS, regardless of their thickness, was significantly decreased in both assays.

Due to the variations between the individual slices, no significant differences were found between the two slice thicknesses, although, after 4 h and 48 h of incubation tendencies of a better metabolic activity in the ATP assay were remarked with 200 µm thick slices. Therefore, in further experiments, a thickness of 200 µm was chosen for the PCHS.

3.1.5. PCHS – effect of cardioplegic solution

Cardioplegic solutions are widely used in cardiovascular surgery to reduce cardiac metabolic demand during surgical procedures (71). Therefore, it was hypothesized to be an alternative to KHB, so the heart was stored in a cardioplegic solution, Custodiol®, after organ removal and was also cut in it. After the cutting process, the PCHS were transported in Custodiol® before being incubated in culture medium. The results are depicted in contrast to the prior results in **Figure 22**.

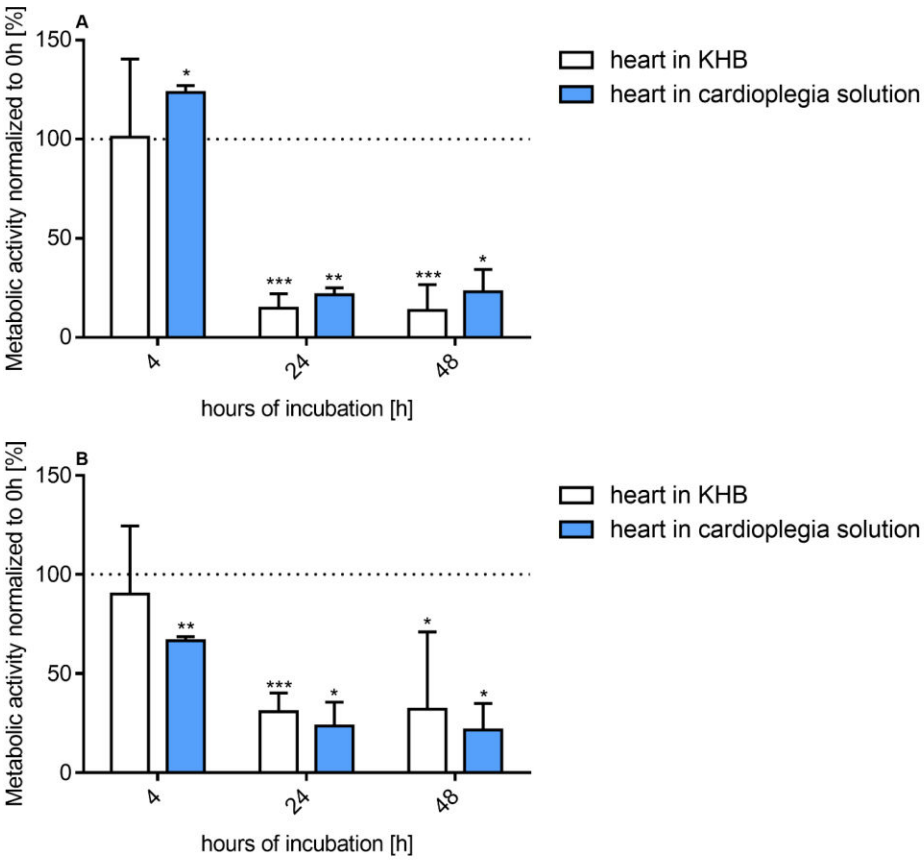

Figure 22: Effect of cutting the heart and storing the heart and PCHS in cardioplegic solution on the metabolic activity of PCHS

The heart was stored in Custodiol®, and cut into PCHS in Custodiol®. The PCHS were then incubated for 4 h, 24 h and 48 h. After the incubation period the metabolic activity of the slices was assessed via ATP assay (A) and MTT assay (B) and normalized to the control before incubation (n=2, N=3). The results of the PCHS stored and cut in KHB were taken from the previous experiment (3.1.4). Depicted as mean + SD. (*: $p \leq 0.05$, **: $p < 0.01$, ***: $p < 0.001$, statistical significance vs. before incubation, unpaired t-test)

Storing and cutting PCHS in KHB did not lead to significant changes after 4h of incubation compared to the non-incubated control, as already shown in **Figure 21**. Storing and cutting PCHS in Custodiol® on the other hand led to a significant increase in metabolic activity after 4 h of incubation when assessed by the ATP assay. The MTT assay on the other hand showed a significant decrease in activity.

After 24 h and 48 h of incubation, PCHS of both conditions showed a significant decrease in metabolic activity compared to the non-incubated control in both assays. Furthermore, there were no significant differences observed between the two experimental conditions.

So, for further experiments, the heart was stored and cut in the less expensive KHB.

3.1.6. PCHS – effect of antioxidant use

Oxidative stress is a major contributor to myocardial damage in the setting of ischemia (131). Therefore, increased expression of antioxidant genes has been suggested to be cardioprotective (131). For this reason, the addition of N-acetylcysteine (NAC) and TEMPOL, two antioxidants, has been hypothesized to improve the metabolic activity of PCHS. **Figure 23** and **Figure 24** depict the effects of NAC and TEMPOL on the metabolic activity of PCHS, respectively.

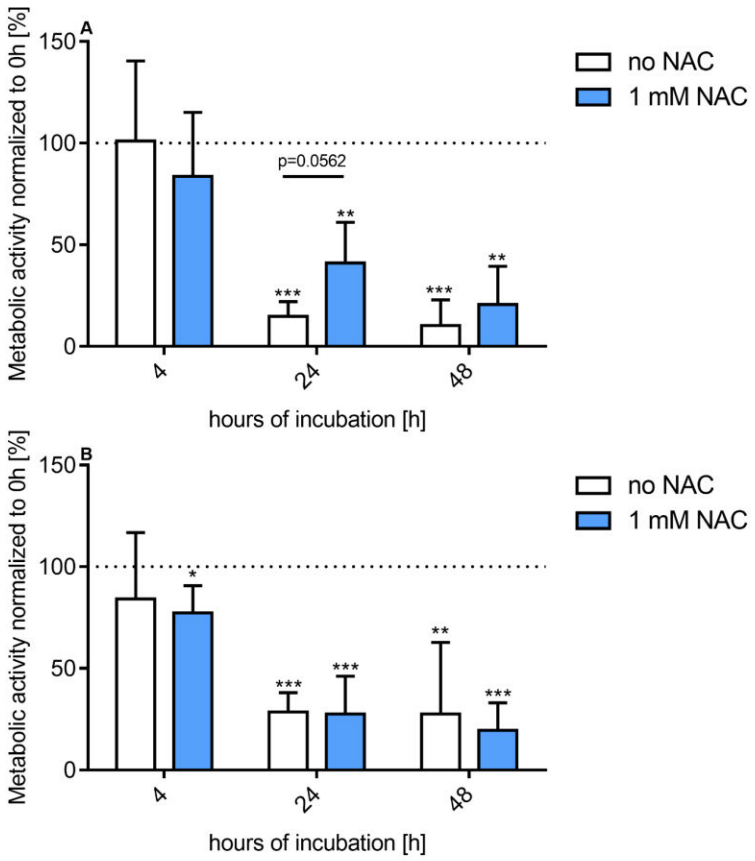

Figure 23: Effect of NAC on the metabolic activity of PCHS

PCHS were incubated for 4 h, 24 h, and 48 h in 1 mM NAC-containing medium. After the incubation period the metabolic activity of the slices was assessed via ATP assay (A) and MTT assay (B) and normalized to the control before incubation (n=3, N=3 (A) and n=4, N=3 (B)). The data of the PCHS incubated without NAC were obtained from the experiment examining the slice thickness of PCHS (3.1.4) in A. In B it was also obtained from 3.1.4 in addition to one new experiment with N=3. Depicted as mean + SD. (*: $p \leq 0.05$, **: $p < 0.01$, ***: $p < 0.001$, statistical significance vs. before incubation, unpaired t-test)

PCHS incubated with NAC exhibited a slight decrease in metabolic activity after 4 h of incubation. This was seen in both assays but was only significant in the MTT assay. This decrease was not present in PCHS without NAC as stated in chapter 3.1.4.

After 24 h and 48 h of incubation, all PCHS with or without the addition of NAC had a decreased metabolic activity in comparison to their activity before incubation. There were no statistically significant differences between the PCHS with or without NAC.

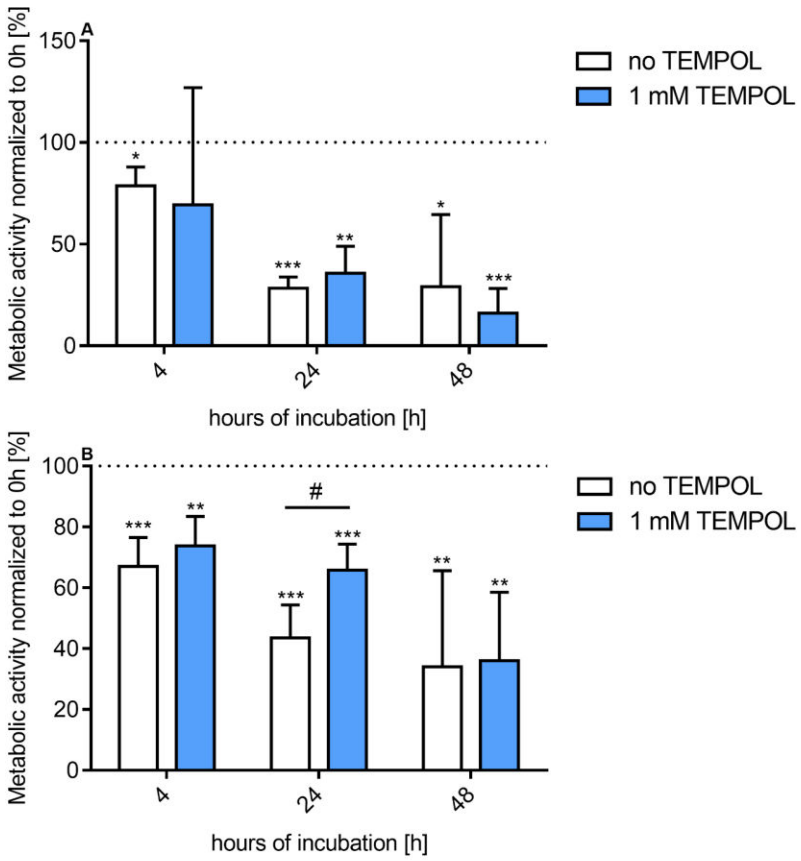

Figure 24: Effect of TEMPOL on the metabolic activity of PCHS

PCHS were incubated for 4 h, 24 h, and 48 h either in medium containing 1 mM TEMPOL or in medium without TEMPOL. After the incubation, the metabolic activity of the slices was assessed via ATP assay (A) and MTT assay (B) and normalized to the control before incubation. In A: n=3, N=3. In B: n=4, N=3 (except once N=2). Depicted as mean + SD. (*: $p \leq 0.05$, **: $p < 0.01$, ***: $p < 0.001$, #: $p \leq 0.05$, asterisks depict statistical significance vs. before incubation, pounds depict statistical significance between two groups, unpaired t-test)

The second evaluation was done with the addition of TEMPOL to the culture medium. Contrary to the experiment above, where an already existing control group was used, in this experiment, the respective control group was incubated together with the treatment groups. The control group incubated without TEMPOL showed a significant decrease after 4 h of incubation in both assays. This was in contrast to prior results (3.1.4), where no significant loss of metabolic activity was observed in the control slices. At every incubation time, both PCHS with and without TEMPOL showed a significantly decreased metabolic activity in both assays, except PCHS incubated with TEMPOL after 4 h of incubation when assessed with the ATP assay.

PCHS incubated with TEMPOL had a significantly higher metabolic activity after 24 h of incubation than those treated without, when assessed in the MTT assay.

3.2. Histological analysis of untreated PCLS

To understand the changes that arise in the PCLS during incubation, the untreated PCLS were analyzed histologically after incubation for 4 h and 24 h. After hematoxylin and eosin (H&E) staining, the nucleus area, nucleus number, and number of binucleated cells were quantified in comparison to PCLS before incubation.

In addition to these quantitative measures, the images were evaluated concerning numerous qualitative differences, too. Representative images of the PCLS before incubation, after 4 h of incubation, and after 24 h of incubation are shown in **Figure 25**. Parts of this figure have been previously published in our preprint (1).

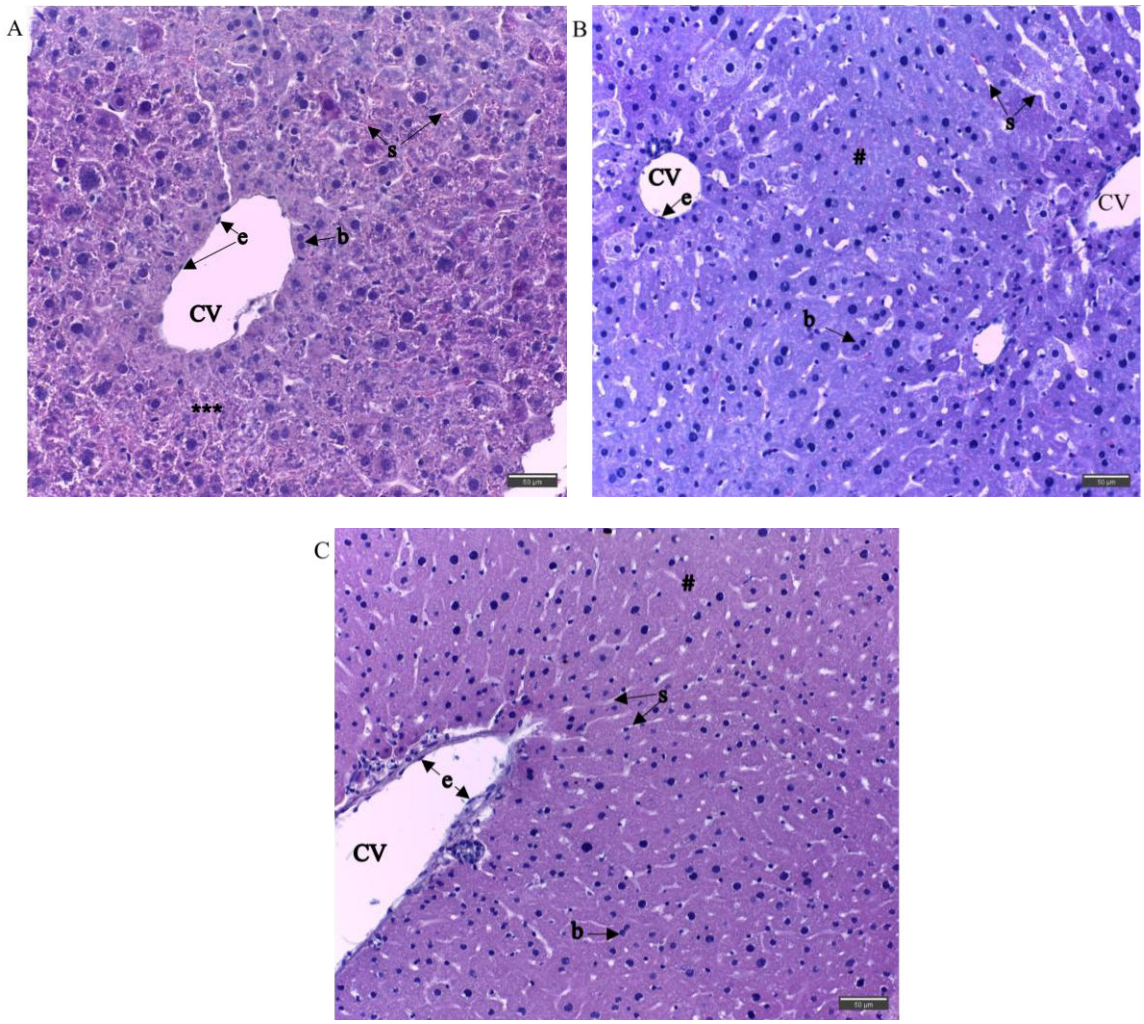

Figure 25: H&E staining of representative non-incubated PCLS, PCLS after 4 h of incubation and PCLS after 24 h of incubation

PCLS were stained with H&E staining and pictures were taken with a Leica DM750 microscope under 200x magnification. A scale bar is depicting a length of 50 µm in the images. A representative image for each time point is shown. A: non-incubated, B: after 4 h of incubation, C: after 24 h of incubation. Important structures are labeled exemplarily as follows. CV: central vein; s: sinusoid; b: binucleated cell; e: endothelium; ***: granular cytoplasm; #: loss of granular cytoplasm

All PCLS exhibited the characteristic microanatomic structure of the liver. The PCLS taken before incubation started, had abundant granular cytoplasm. While this was already lost by 4 h of incubation. An apparent loss of nucleus area (**Figure 26**) as well as the occurrence of binucleated hepatocytes (**Figure 27**), a marker of liver regeneration, was analyzed.

3.2.1. Analysis of nucleus area and nucleus number in PCLS

The images of the H&E-stained PCLS were analyzed for their nucleus area and nucleus number (**Figure 26**).

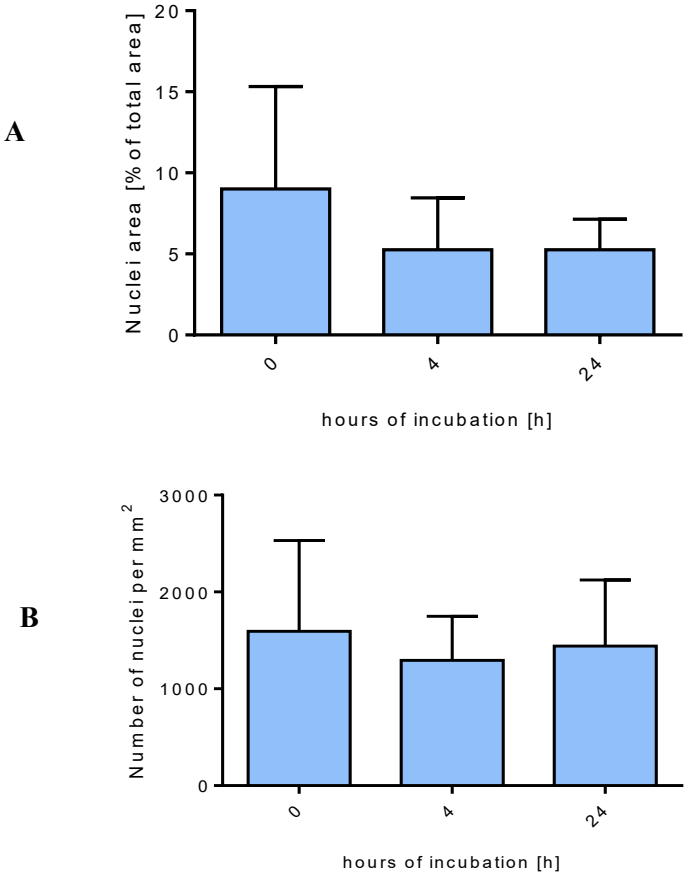

Figure 26: Change in nucleus area and nucleus number in PCLS over incubation time

PCLS were incubated for 0 h, 4 h and 24 h. After incubation, the PCLS were fixed in formalin and H&E-staining was performed. Pictures of the H&E-stained slices were analyzed in Fiji 2.9.0. for their nucleus area (A) or nucleus number (B). The nucleus area or nucleus number was then related to the total tissue area in the picture. as mean + SD: n=4, N=5. (unpaired t-test vs. before incubation)

While at the beginning of the incubation period, the area of the nuclei made up about 8 % of the slice, it was tendentially decreased after 4 h and 24 h of incubation without reaching significance. Furthermore, there was no significant change in nucleus number in the PCLS over the incubation time.

3.2.2. Analysis of the number of binucleated cells in PCLS

The images of H&E-stained PCLS were analyzed for the abundance of binucleated cells. The results are depicted in **Figure 27**.

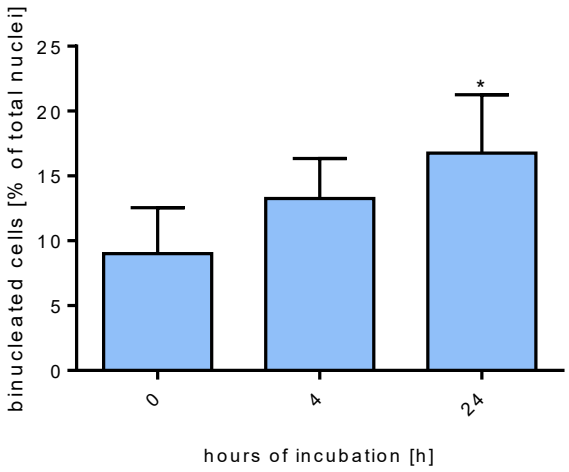

Figure 27: Change in the number of binucleated cells in PCLS over incubation time

PCLS were incubated for 0 h, 4 h and 24 h. After incubation, the PCLS were fixed in formalin and H&E-staining was performed. Pictures of H&E-stained slices were analyzed in Fiji 2.9.0. for the number of binucleated cells. The binucleated cells were then related to the total number of nuclei in the picture. Depicted as mean + SD: n=4, N=5. (*: $p \leq 0.05$, statistical significance vs. before incubation, unpaired t-test)

It was found that with a longer incubation period, the PCLS showed an increased number of binucleated cells. While the increase was not significant after 4 hours, it was significant after 24 hours of incubation.

3.3. RT-qPCR of untreated PCLS

The expression of biotransformation enzymes in the liver was tested via RT-qPCR. This included the CYP-enzyme coding genes of Cyp1a1, Cyp2e1, Cyp2c29 and Cyp3a11, as well as the genes of phase II conjugating enzymes: Gsta3, Ugt1 and Sult1c2. Their relative expression after 4 h of incubation in comparison to before incubation is depicted in **Figure 28**.

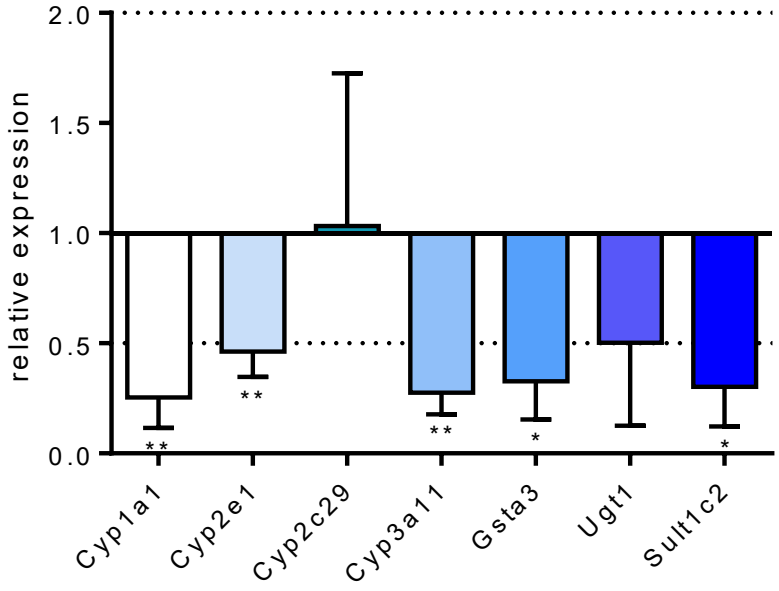

Figure 28: mRNA expression of genes of selected enzymes after 4 h of incubation relative to β-actin and Gapdh expression

PCLS before incubation and PCLS 4 h after incubation were collected and tested for selected biotransformation enzymes using RT-qPCR. The expression was normalized to β-actin and Gapdh expression. And each mRNA's expression was compared to its value before incubation. Depicted as mean + SD: n=3, N=1. (*: $p \leq 0.05$, **: $p < 0.01$, statistical significance vs. before incubation, unpaired t-test)

It was observed that the mRNA of almost all biotransformation enzymes tested was downregulated, except that of Cyp2c29. The reduced expression reached significance in all downregulated genes, except Ugt1.

3.4. Effect of treatment on PCLS

Next, the PCLS were treated with selected pharmacologic compounds and the PCLS were tested for metabolic activity using MTT and ATP assays after incubation for 4 h and 24 h, respectively. The histological changes were assessed by H&E staining. The effects on metabolic activity are summarized below. The histological changes are presented in summary at the end of this chapter.

3.4.1. Acetaminophen treatment

Acetaminophen treatment was assessed after an incubation period of 4 h and 24 h. At 4 h after incubation, only 1 mM, 5 mM and 10 mM were tested in addition to a control group without acetaminophen. 24 h after incubation, a broader range of concentrations between 1 mM and 10 mM was included in the evaluation. The effects of the

acetaminophen treatment are shown in **Figure 29**. A modified version of this figure was previously published in our preprint (1).

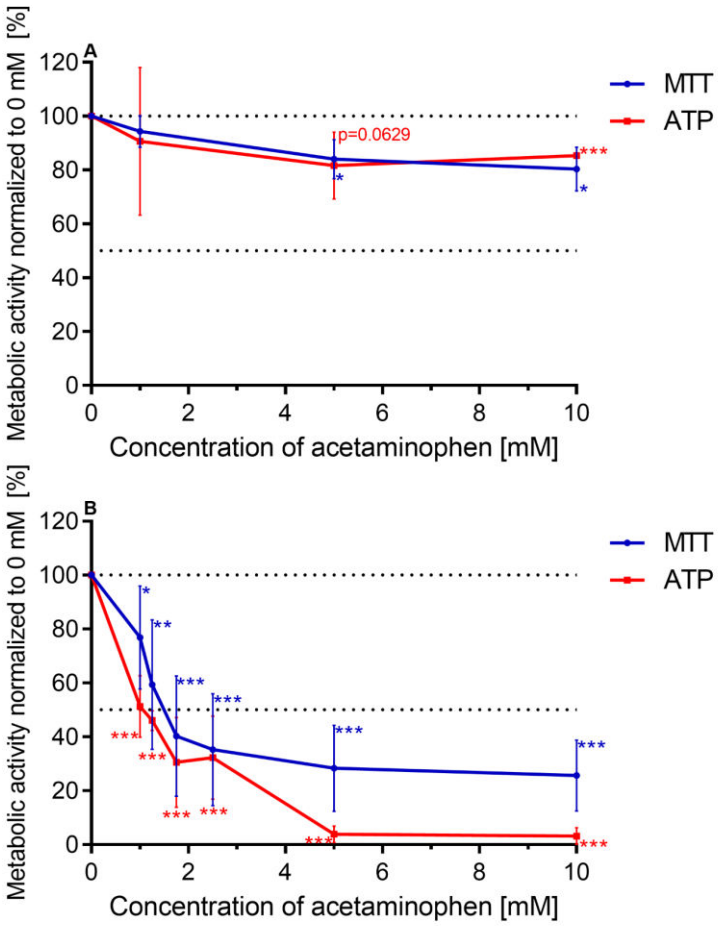

Figure 29: Effect of acetaminophen treatment on the metabolic activity of PCLS

PCLS were incubated for 4 h (A) and 24 h (B) in a medium that contained increasing concentrations of acetaminophen. After the incubation, the PCLS were evaluated for their metabolic activity using ATP assay and MTT assay. The metabolic activity was normalized to the control incubated without acetaminophen. A: n=3, N=3. B: Technical replicates were always used at N=3. The evaluation after 24 h was originally started with the same concentrations as in A, but later, further concentrations of acetaminophen were added for a more detailed evaluation. This led to the following test numbers, ATP: 0 mM n=7, 1 mM n=7, 1.25 mM n=3, 1.75 mM n=4, 2.5 mM n=4, 5 mM n=6, 10 mM n=6; MTT: 0 mM n=7, 1 mM n=7, 1.25 mM n=3, 1.75 mM n=4, 2.5 mM n=5, 5 mM n=6, 10 mM n=5. Depicted as mean + SD: (*: $p \leq 0.05$, **: $p < 0.01$, ***: $p < 0.001$, statistical significance vs. untreated control, unpaired t-test)

The PCLS exhibited a slight but concentration-dependent decrease in metabolic activity after 4 h of incubation. The loss of metabolic activity was significant from 5 mM acetaminophen. Despite increasing concentrations, the PCLS remained at about 80 % of their metabolic activity.

A concentration-dependent decrease in metabolic activity was also observed after 24 h of incubation. However, the slices reacted more sensitively to acetaminophen than after

4 h of incubation and the loss of metabolic activity was already significant at 1 mM acetaminophen. While the metabolic activity in the MTT assay stabilized at about 30 % despite increasing concentrations, it continued to decrease in the ATP assay and almost completely disappeared at 5 mM acetaminophen.

In addition, the color of the PCLS changed after 24 h of treatment with acetaminophen as depicted in **Figure 30**.

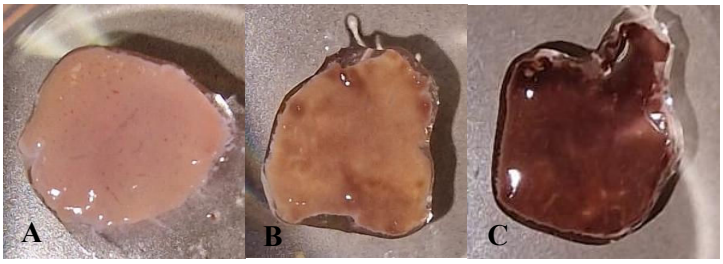

Figure 30: Color change of PCLS after 24 h of acetaminophen treatment

A: no acetaminophen, B: 1.5 mM, C: 5 mM

The IC_{50} of acetaminophen in the PCLS after 24 hours of incubation was 1.0 mM (ATP assay) and 1.3 mM (MTT assay).

3.4.2. Cisplatin treatment

Cisplatin concentrations of 10 µM, 30 µM, and 100 µM were used and compared to a control group without cisplatin. The evaluation of the metabolic activity of the PCLS is shown in **Figure 31**. A modified version of this figure was previously published in our preprint (1).

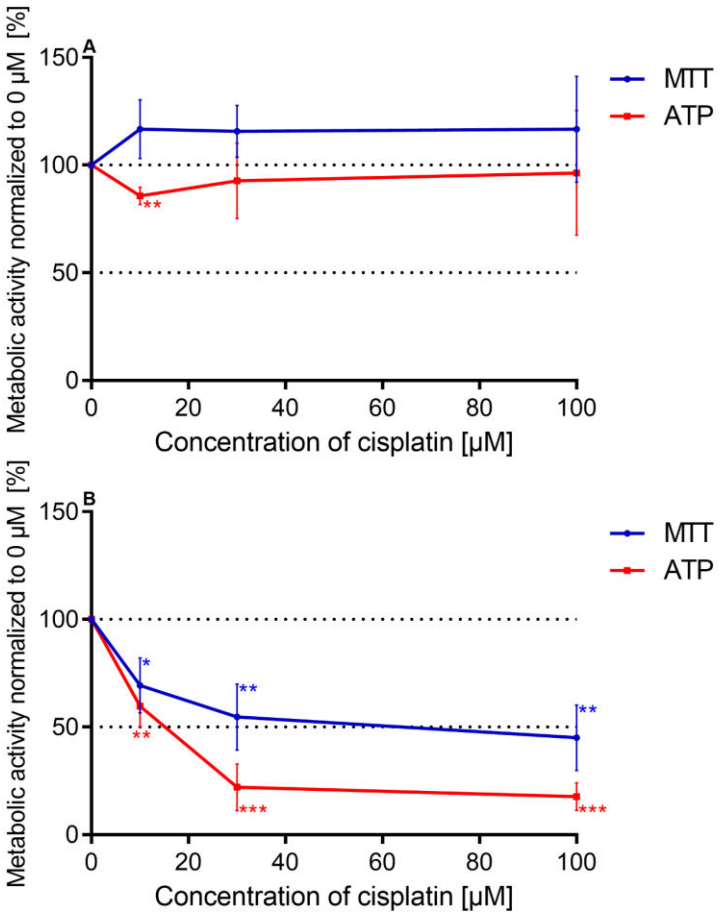

Figure 31: Effect of cisplatin treatment on the metabolic activity of PCLS

PCLS were incubated for 4 h (A) and 24 h (B) in a medium that contained increasing concentrations of cisplatin. After the incubation, the PCLS were evaluated for their metabolic activity using ATP assay and MTT assay. The metabolic activity was normalized to the control incubated without cisplatin. Depicted as mean + SD: n=3 N=3 (*: $p \leq 0.05$, **: $p < 0.01$, ***: $p < 0.001$, statistical significance vs. untreated control, unpaired t-test)

After 4 h of incubation, the PCLS had an insignificant rise in metabolic activity in the MTT and a loss in the ATP assay. Only the decrease in activity seen with 10 µM cisplatin in the ATP assay was significant.

After 24 h of incubation, however, the PCLS displayed a dose-dependent decrease in metabolic activity. The decrease was already significant from 10 µM cisplatin. It was also found that the ATP assay showed a higher decrease than the MTT assay.

The IC_{50} of cisplatin in PCLS was12.7 µM (ATP assay) and 56.7 µM (MTT assay) after 24 h of incubation.

3.4.3. Isoniazid treatment

Isoniazid was added in increasing concentrations (0.02 mM, 0.1 mM, 0.25 mM, 0.5 mM, 1 mM, 1.5 mM, and 5 mM) to the medium. The PCLS were then incubated in it for 4 h and 24 h. The effect of isoniazid on metabolic activity is shown in **Figure 32**.

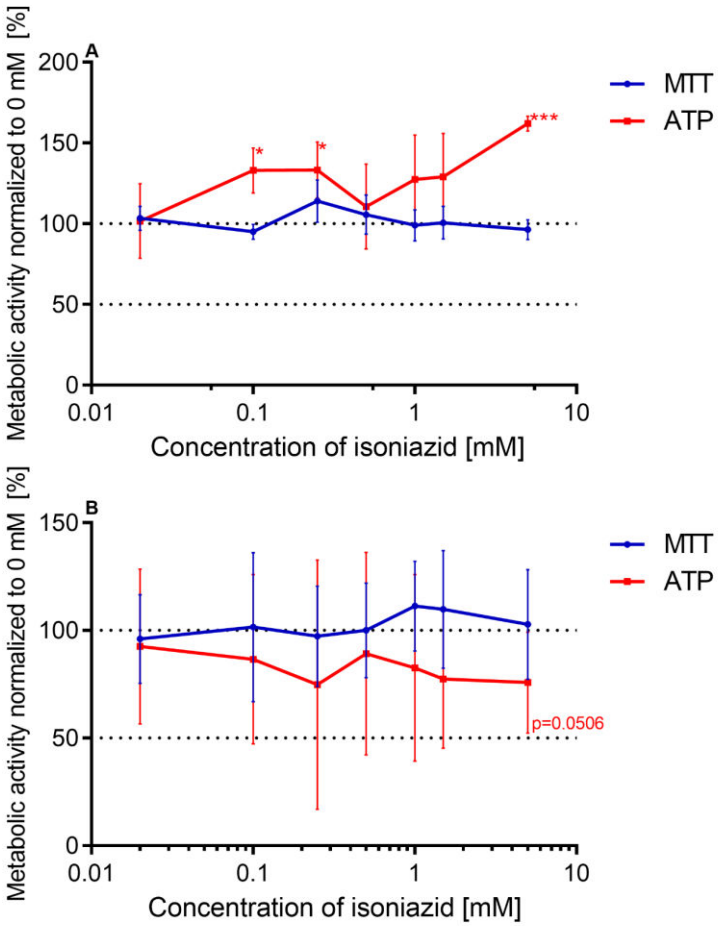

Figure 32: Effect of isoniazid treatment on the metabolic activity of PCLS

PCLS were incubated for 4 h (A) and 24 h (B) in a medium that contained increasing concentrations of isoniazid. After the incubation, the PCLS were evaluated for their metabolic activity using ATP assay and MTT assay. The metabolic activity was normalized to the control incubated without isoniazid. A: n=3 N=3. B: ATP: n=5 N=3 except 0.02 mM n=4, 5 mM n=4; MTT: n=4 N=3. Depicted as mean + SD on a logarithmic x-axis: (*: $p \leq 0.05$, ***: $p < 0.001$, statistical significance vs. untreated control, unpaired t-test)

After 4 h of incubation, a concentration-dependent increase in the metabolic activity of the PCLS was recorded using the ATP assay. This was significant at concentrations of 0.1 mM, 0.25 mM, and 5 mM. In contrast, the MTT assay showed no significant changes in metabolic activity with increasing isoniazid concentrations.

After 24 h of incubation, the PCLS in the ATP assay displayed a slight tendency to decrease in metabolic activity with increasing isoniazid concentrations. Statistical

analysis showed a difference of p=0.0506 at 5 mM isoniazid. However, the MTT assay, revealed no significant differences.

3.4.4. Melatonin treatment

Melatonin was tested in the concentrations of 20 µM, 60 µM, and 200 µM. The PCLS were incubated for 4 h and 24 h. The effect of melatonin on the metabolic activity of the PCLS is shown in **Figure 33**. A modified version of this figure was previously published in our preprint (1).

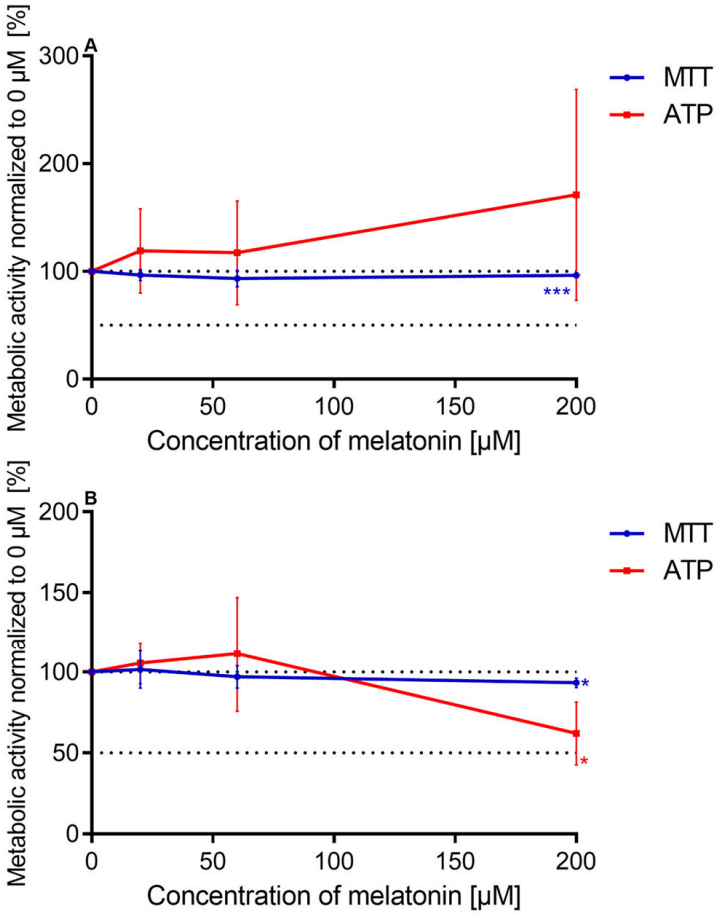

Figure 33: Effect of melatonin treatment on the metabolic activity of PCLS

PCLS were incubated for 4 h (A) and 24 h (B) in a medium that contained increasing concentrations of melatonin. After the incubation, the PCLS were evaluated for their metabolic activity using ATP assay and MTT assay. The metabolic activity was normalized to the control incubated without melatonin. Depicted as mean + SD: n=3 N=3 (*: $p \leq 0.05$, ***: $p < 0.001$, statistical significance vs. untreated control, unpaired t-test)

After 4 h of incubation, the PCLS showed a tendency towards a concentration-dependent increase in metabolic activity, as determined by ATP assay. However, this increase was not statistically significant. The MTT assay indicated almost no

differences. At 200 µM melatonin, though, the metabolic activity was 96 % which was calculated to be statistically significant.

After 24 h of incubation, the PCLS displayed no change in metabolic activity at 20 µM or 60 µM of melatonin. A significant decrease was observed when incubated in 200 µM of melatonin. This was less pronounced in the MTT assay than in the ATP assay.

3.4.5. Histological changes after treatment in PCLS

The PCLS were analyzed for their nucleus number and amount of binucleated cells after 4 h and 24 h of incubation. **Figure 34** displays the change in nucleus number in the different treatments, while **Figure 35** displays the change in the amount of binucleated cells.

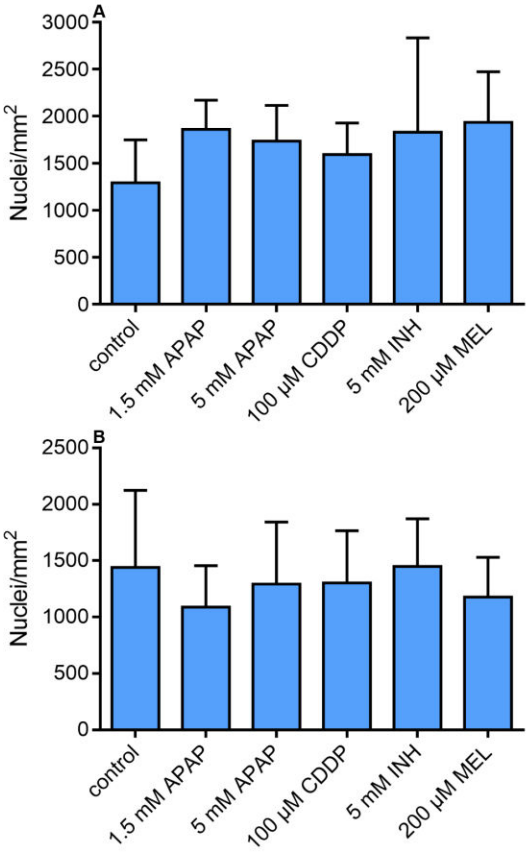

Figure 34: Change in nucleus number in PCLS with treatment

PCLS were treated with acetaminophen (APAP), cisplatin (CDDP), isoniazid (INH), and melatonin (MEL) for 4 h (A) and 24 h (B). The PCLS were then fixed in formalin and H&E-stained. The nucleus number was evaluated in Fiji 2.9.0. and related to the total area. Depicted as mean + SD. (not significant vs. control, unpaired t-test)

After 4 h of incubation with the different substances, the PCLS had a slight tendency to increase the relative nucleus number. After 24 h of treatment, a slight tendency towards

a decreased relative nucleus number was observed for most substances. However, these trends were not significant.

In addition, the number of binucleated cells in the PCLS was analyzed for changes caused by different treatments. The results are shown below.

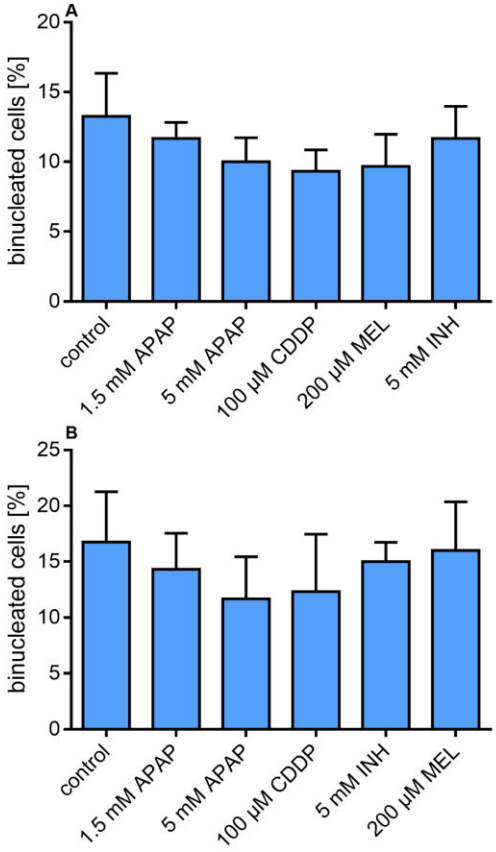

Figure 35: Change in the number of binucleated cells in PCLS with treatment

PCLS were treated with acetaminophen (APAP), cisplatin (CDDP), isoniazid (INH), and melatonin (MEL) for 4 h (A) and 24 h (B). The PCLS were then fixed in formalin and H&E-stained. The binucleated cells were evaluated in Fiji 2.9.0. and related to the total nuclei number. Depicted as mean + SD. (not significant vs. control, unpaired t-test)

The PCLS treated with acetaminophen, cisplatin, and isoniazid tended to have fewer binucleated cells after 4 h and 24 h of incubation than the control. Nevertheless, this was not statistically significant.

4. Discussion

Some of the data and findings discussed in this chapter were previously included in our preprint (1).

4.1. Effect of incubation on untreated PCLS

One objective of this thesis was to characterize the effect of different incubation conditions on PCLS. This would allow a better understanding of the influence of the incubation itself on PCLS viability. Optimal culture conditions for PCLS were desirable in order to maximize the validity of the toxicity studies planned for later.

4.1.1. Overall viability

The results have shown that the metabolic activity of incubated PCLS, a marker for overall PCLS viability, decreased over time. Although the exact values differed between the viability assays and between the individual experiments, a clear downward trend was observed over time. When comparing the two viability assays that were used, the ATP was generally more sensitive than the MTT assay regarding decreases in metabolic activity. The decreases in metabolic activity observed after 48 h of incubation were more pronounced in the ATP assay than in the MTT assay. Generally, metabolic activity after 48 h was estimated to be around 10 % - 30 % of the values before incubation in the ATP assay, while it was estimated to be around 50 % - 80 % when the MTT assay was used. The rapid decline in PCLS viability limits the use of PCLS to the research of acute cellular reactions and may make the study of chronic toxicity impossible if the lifetime of PCLS cannot be extended.

It is challenging to compare these values to other publications since published viabilities have often been normalized to an incubated control group rather than to values before incubation (132). However, two papers, from 2015 and 2017 respectively, reported to have observed stable ATP concentrations in PCLS of rats up to 96 h and 120 h (133, 134). Although this sounds promising, it differs from the data observed in this thesis. Comparing the data obtained from previous research on rat PCLS and the data observed in this thesis might be limited due to interspecies differences, though. Within our workgroup, continued work with murine PCLS observed similar results to those documented in this thesis. This demonstrated the reproducibility of results between different experimenters (1).

Due to the limitation in possible incubation time, the viability of the PCLS after 24 h of incubation was selected to be the main data point to be evaluated when the PCLS were treated with acetaminophen, cisplatin, isoniazid, and melatonin. In this regard, it was aimed to maximize the viability of the PCLS during the 24 h of incubation, as they served as the control group. For reference, the MTT assay estimated the viability of the PCLS to be around 80 % - 100 % of their value before incubation with little variability throughout the different experimental conditions. On the other hand, the viability estimates made with the ATP assay were lower, at around 40 % - 80 %, and had a high variation. For comparison, a previous work that used ATP measurements for viability estimation reported murine PCLS to be 71 % active after 24 h of incubation (39). Similarly, rat PCLS were observed to 83 % active after 24 h of incubation (135). These viability estimates regarding the 24-hour mark are within the range of the observations presented in this thesis. This consistency demonstrates the reproducibility of the results across different PCLS models.

A striking result that was repeatedly noticed in a lot of the experiments presented in this thesis was the initial increase in metabolic activity after 4 h of incubation. These were most pronounced in the MTT assay. A possible explanation for this increase is a stress response of the cells to the slicing process. Analogous to this, an initial increase in LDH leakage was observed in PCLS of rats and mice in previous works (133, 136). As the slicing process damages cells, an increase in LDH, a direct marker of cell damage, is to be expected (133). One can assume that this damage is a source of cellular stress for the tissue that could trigger a stress response. It has been described that the MTT reduction rate is increased extra-mitochondrially when glycolysis is stimulated (137). Oxidative stress was shown to be one source of glycolysis stimulation in hepatoma cells (138). This could be an explanation as to why the increase was more pronounced in the MTT assay, rather than the ATP assay. Therefore, this peak in activity was considered to be a sign of a cellular stress response. A pronounced increase in activity after 4 h of incubation was considered not desirable in the evaluation of the experiments.

4.1.2. Histology and PCR

Histological evaluation was performed in PCLS incubated up to 24 h. The microanatomical structure of the liver was observed to be generally intact in the H&E stainings of the PCLS. However, the tissue lost its granular cytoplasm and showed some signs of necrosis after 24 h of incubation. This is consistent with previous reports, that

observed first necrotic signs after 12 h of incubation (139). Quantitative analysis of the nuclei in the PCLS was also performed. The performed analysis showed a tendency towards loss in nucleus area, and a significant increase in the number of binucleated cells after 24 h of incubation. Considering the aforementioned decrease in ATP concentration and the fact that necrotic cells lose their nuclei, the observed decrease in relative nucleus area in the PCLS is probably a sign of beginning necrosis (140). Overall, while the PCLS were generally histologically intact, necrotic processes seemed to have started already. This aligned with the decrease in metabolic activity seen in the viability assays. However, the observed increase in the number of binucleated liver cells might demonstrate an example of vital liver functions. An increase in binucleated cells has also been described as a reaction to tissue injury in the liver regeneration process (141). An increase in binucleated cells was also seen in the regenerative process of partial hepatectomies (141). This implies that the cellular response of PCLS to the slicing process may be analogous to a partial hepatectomy. Similarly, a study from 2015, that observed PCLS after 120 h of incubation, reported cell proliferation in the PCLS (133). This means that although the overall viability of the PCLS decreased, they may still have regenerative properties.

The performed RT-qPCR showed that the mRNA of various phase I and phase II biotransformation enzymes was downregulated after 4 h of incubation. These biotransformation enzymes play an important role in the function of the liver. A decrease in their expression imposes a possible restriction of PCLS use, especially in the fields of pharmacology and toxicology. In many cases, the toxicity of a substance is induced or terminated by metabolic reactions in the liver. A decrease in mRNA expression does not necessarily restrict the protein expression simultaneously, though (142). Human CYP enzymes have a half-life of 24 h to 140 h *in vitro* (143). The protein levels and their activity are better parameters to estimate hepatic function. The viability decrease in the PCLS with APAP treatment indicated APAP metabolization to NAPQI, and therefore demonstrated persistent hepatic function in PCLS in spite of mRNA downregulation, since NAPQI is formed by CYP450 enzymes. Additionally, it is worth noting that in this thesis the mRNA expression of only seven metabolic enzymes was tested. Of the seven enzymes that were tested, Cyp2c29 was not downregulated. Similarly, other enzymes that were not tested here might not be downregulated as well. The differences in the expression of certain CYP enzymes were previously described in rat PCLS in which it was seen CYP2B1 and CYP3A2 were better expressed than

CYP1A1 (144). The decrease in mRNA concentration is of value though, as it demonstrates an impairment in cellular function in the PCLS.

4.1.3. Incubation conditions

To optimize the viability of PCLS during incubation, the effect of different slice thicknesses was tested. The slice thickness is an important characteristic of PCLS. Thinner PCLS allow a better diffusion of oxygen at the expense of an increased ratio of damaged cell layers to undamaged ones (145). 200 µm, 250 µm, and 300 µm thick PCLS were used for this assessment. Previously, it has been suggested to use 250 µm thick PCLS (23). However, all three thicknesses have been used in PCLS protocols throughout the years (145, 146). No significant differences were found when comparing the three slice thicknesses regarding their effects on the viability of PCLS using MTT and ATP assays. This indicates that the slice thickness does not effect the viability in this thickness range. This is beneficial for the implementation of PCLS in scientific research, as it indicates that PCLS remain comparable in this thickness range.

Next, the glucose content of the incubation medium was evaluated. PCLS were incubated in a low-glucose medium (11 mM) and a high-glucose medium (25 mM). While 25 mM glucose is a supra-physiologic glucose concentration level, 11 mM is closer to the physiologic intrahepatic glucose concentration (130). Previously, different glucose concentrations have been used to incubate PCLS. Among those were 11 mM (147), 14 mM (23), and 25 mM (148) glucose-containing media. The viability of the PCLS assessed with MTT and ATP assays did not reveal any significant differences between the two glucose concentrations used. This again shows that the viability of PCLS remains comparable even with different incubation protocols. As different workgroups will have some variations in their incubation protocols, it is advantageous that the viability of PCLS is not easily affected by changing conditions. While this cannot be generalized to all protocol differences, it may be a hint at the reproducibility of the method. Furthermore, it is a benefit that the lower glucose concentration is sufficient for the culture of PCLS, since higher concentrations might exert additional effects and potentially interfere with subsequent experiments.

Another method that has been used to enhance the incubation medium is its saturation with carbogen (95 % O_2, 5 % CO_2) (149). For this, PCLS were cut in carbogen-gassed KHB and incubated in carbogen-gassed medium. This was compared to ungassed conditions. A significant difference was observed when tested with the MTT assay. The

activity of the ungassed PCLS was higher after 4 h and 24 h of incubation. Although there was no clear explanation, the higher oxygen concentration in the carbogen might have increased oxidative radicals in the gassed PCLS (150), and therefore effected this group negatively. When assessed with the ATP assay, no differences between the two groups were observed. To avoid oxidative stress in the PCLS ungassed conditions were further used.

4.2. Effect of incubation on PCHS

Another objective of this thesis was to characterize the effect of different incubation conditions on PCHS. First, the effect of slice thickness on the viability of PCHS was assessed. 200 µm and 250 µm thick PCHS were compared using the ATP and MTT assays. After 4 h of incubation, 200 µm thick PCHS performed slightly better in both viability assays, although it was not statistically significant. This may be explained by the higher oxygen diffusion in thinner slices. However, there was no difference between the two thicknesses after 24 h of incubation. While 300 µm thick porcine PCHS were used in a previous work (43), mouse hearts were too small for such slices. In practice, this makes it necessary to produce thinner PCHS. This increases the number of PCHS that can be produced from the limited-sized murine hearts.

As with the PCLS, the viability of PCHS decreased over time. The decrease in viability was much faster in PCHS, though. While after 4 h of incubation, the viability of the PCHS was still consistently measured to be above 50 %, this was not the case after longer incubation periods. This was expected, as the heart tolerates ischemia less than the liver (70). Nevertheless, this severely restricts the applicability of PCHS.

However, the results must be judged cautiously. The experiments with PCHS were significantly limited by the size of the organ. Unlike the liver, the heart was not large enough to produce satisfying amounts of PCTS. The precalculated sample size that was needed for the experimental design was not always met and often needed significant adjustments. This decreased the reliability of the method and has to be kept in mind when interpreting the results.

Next, the solution, in which the heart was sliced, was changed. Slicing the heart in KHB was compared to slicing it in a cardioplegic solution. It was hypothesized that the reduction of metabolic demand by cardioplegia would have a protective effect on the myocardium (71). Although, KHB has been described to be the best solution to perfuse

isolated hearts (151). After 24 hours of incubation, there were no significant differences in viability of PCHS in the two solutions. After 4 h of incubation, the PCHS cut in a cardioplegic solution tended to perform better when evaluated using the ATP assay, while they tended to perform worse when evaluated using the MTT assay. The differences were not significant. Recently, another protocol using BDM-supplemented Tyrode's solution demonstrated retained viability and contractility in pig heart slices (152). It can be hypothesized that similar changes to protocol may have positive effects on the viability of mouse PCHS as well, and may be tested in future evaluations of PCHS viability.

Next, antioxidants (NAC or TEMPOL) were added to the incubation medium of the PCHS, and their effect on the viability of PCHS was measured using ATP and MTT assays. Strikingly, both antioxidants improved the viability of the PCHS after 24 h of incubation, with the effect of TEMPOL reaching statistical significance. The improvement with NAC was observed in the ATP assay, while the improvement with TEMPOL was observed in the MTT assay. The positive effects of antioxidants might indicate that the previously observed decrease in the viability of PCHS was linked to oxidative stress. Therefore, PCHS incubation might be optimized by further addition of antioxidants in the future. In particular, a combination of different antioxidants such as NAC and TEMPOL could be considered, as this may provide complementary protection and further enhance viability. Other possible future additions to PCHS incubation may be electrical stimulation and the addition of growth factors, as they have been tested successfully on porcine PCHS (43).

Overall, the incubation of PCHS had limitations. The aforementioned size of the organ and the high variability in its data outcome were the main problems in the use of murine PCHS. Bigger animals, such as rats or pigs, might be more suitable to produce PCHS in the future. The approach of adding antioxidants to the medium was promising though.

4.3. Treatment of PCLS

4.3.1. Acetaminophen treatment

To assess the tissue’s reaction, the PCLS were treated with pharmacological substances. Because the use of PCLS aims to serve as an *ex vivo* alternative for *in vivo* experiments, the model aims to provide physiologically relevant and translatable information for further *in vivo* considerations. First, treatment with acetaminophen (APAP) was initiated, since APAP is a well-known hepatotoxin.

After 4 h of incubation a mild decrease in viability was observed with high-dose APAP treatment. However, a clear concentration-dependent decrease in viability was only observed after 24 h of incubation. After 4 h of incubation, the viability estimates of both used assays were similar to each other. After 24 h of incubation though, the decrease in viability was more pronounced in the ATP assay. This reflects that the ATP assay seemed to be more sensitive to changes in viability in the PCLS. The marked concentration-dependent decrease in PCLS viability, observed with both viability assays, is a good indicator that the PCLS accurately reproduce the hepatotoxic effects of APAP. APAP causes intrinsic DILI which is characterized by a marked concentration-dependent toxicity (75). The reproducibility of APAP-toxicty in PCLS also demonstrates retained cellular function in the PCLS. First of all, viable cells are necessary to allow APAP toxicity (153). As discussed in chapter 4.1.2, to reproduce APAP toxicity, the hepatic metabolization of APAP must be conserved long enough to produce sufficient amounts of the toxic metabolite NAPQI. This reaction seen in PCLS to the model-compound of APAP indicates the applicability of PCLS to assess pharmacotoxicology.

A previous study that was conducted on rat PCLS, described a concentration-dependent decrease in viability at a concentration of 10 mM APAP (135). In the experiments conducted in this thesis, 10 mM APAP already had significant toxic effects on the murine PCLS. This corresponds exactly to the *in vivo* conditions as rats are less susceptible to APAP toxicity than mice (154).

The calculated IC_{50} for APAP after 24 h was 1.0 mM (ATP assay) and 1.3 mM (MTT assay). The IC_{50} values calculated from the data of the two viability assays were very close to each other. This indicates that, at least in the case of APAP, both methods are reliable alternatives. A previous work described an IC_{50} of 3.8 mM in murine hepatocyte cultures with the MTT assay (155). The lower IC_{50} in PCLS may indicate that PCLS are more sensitive toward APAP toxicity than traditional hepatocyte cultures. For reference, targeted therapeutic ranges of APAP in humans are plasma concentrations between 5 to 20 µg/mL (0.033 to 0.132 mM) (156).

In addition, the color of the PCLS changed with APAP treatment after 24 h of incubation. Increasing APAP concentrations caused darker discoloration of the PCLS. This darker discoloration in response to APAP has been described previously with rat PCLS as well (135). Although the exact reason for the color was not described yet, it is

striking that the same color was not seen with other substances and was specific to APAP. Therefore, it might be correlated to a buildup of specific coloured metabolites.

While the number of nuclei was not affected by APAP treatment, the number of binucleated cells tended to decrease. This indicates that APAP inhibited the regenerative response previously described in the PCLS. Due to beginning necrosis, one would have expected a decrease in nuclei number as well. Therefore, it may be useful to assess the number of nuclei again after 48 h of incubation to obtain clearer results. The negative effect of APAP toxicity on the regenerative capacity of the liver has been described previously and is therefore consistent with the data of this thesis (157).

4.3.2. Cisplatin treatment

Next, the PCLS were treated with cisplatin (CDDP) and assessed for their relative change in viability. After 24 h of incubation, the viability of the PCLS decreased when treated with increasing concentrations of CDDP. This decrease was more pronounced in the ATP assay, which demonstrates the sensitivity of the method again. This is also reflected by the calculated IC_{50} values of 12.7 µM (ATP assay) and 56.7 µM (MTT assay). After 4 h of incubation though, no clear trend was observed yet. With the ATP assay, a slight decrease in activity was observed after 4 h of incubation, while with the MTT assay, a slight increase in activity was observed after 4 h of incubation. As already discussed in chapter 4.1.1, this may be explained by oxidative stress caused by CDDP.

Similarly, to APAP treatment, the measured concentration-dependent decrease in the viability of PCLS after 24 h of incubation was in accordance with the expected toxic response. Therefore, APAP and CDDP were good and accurate examples of toxic reactions that could be reproduced with PCLS after 24 h of incubation. When PCLS were examined histologically after CDDP treatment, the number of nuclei was not affected, while the number of binucleated cells tended to decrease. This indicates that CDDP inhibited the regenerative response of the PCLS, as was expected.

Comparing the calculated IC_{50} to previous data is challenging since most experiments conducted with cell cultures used human hepatocyte lines. Therefore, the interspecies variability has to be kept in mind. Nevertheless, the IC_{50} of CDDP in HepG2 cells was calculated to be 39.9 µM which is located between the IC_{50} values calculated from both viability assays. Therefore, the IC_{50} of PCLS is comparable to the data observed in commonly used cell culture models (158).

4.3.3. Isoniazid treatment

The third hepatotoxin used to treat the PCLS was INH. The effect of INH on PCLS viability was not as clear as with the first two substances. With the MTT assay no concentration-dependent viability differences were observed at any of the incubation times that were tested. The ATP assessment presented no clear pattern either. An increase in metabolic activity was observed after 4 h, and a slight decrease in metabolic activity was observed after 24 h of incubation. The measurements also had higher variations. In the histological evaluation, there were no significant effects observed either. So altogether, the hepatotoxic effect of INH was not able to be reproduced with the PCLS.

But this difference in reaction to INH compared to APAP or CDDP is plausible. While INH is hepatotoxic, it is known to cause idiosyncratic DILI in contrast to intrinsic DILI (100). INH toxicity has been hypothesized to be at least partially caused by the production of toxic metabolites (101, 102), therefore INH toxicity is conveyed indirectly. The reproducibility of INH toxicity was always challenging in animal models (100). Therefore, the lack of INH toxicity in PCLS was expected and demonstrates that PCLS and *in vivo* models behave comparably to each other.

4.3.4. Melatonin treatment

Melatonin treatment was used as a negative control on PCLS in the setup of the experiments because no hepatotoxic effects were expected with it. As already discussed earlier (chapter 1.6.4), melatonin is described to have hepatoprotective properties (110, 111, 112).

Melatonin concentrations of up to 200 µM were tested. For reference, the peak serum concentration of melatonin after administration of 100 mg melatonin was described to be 435 nM (159). With 200 µM of melatonin a statistically significant decrease in metabolic activity was observed after 4 h and 24 h of incubation with the MTT assay. This was not thought to be of biological significance though, as the effect was very small in scale (< 5 %). The statistical significance was calculated mathematically due to a limited variation in the results (n=3). After 24 h of incubation, a decrease in metabolic activity was observed in the ATP assay with 200 µM of melatonin, though. This was contrary to expectations. Research on the literature on this topic did not yield any data on the potential hepatotoxicity of melatonin. 100 µM of melatonin was described to reduce the ROS production seen with APAP toxicity in murine hepatocyte cultures

(112). While it is possible that 200 µM of melatonin had negative effects on the viability of the incubated PCLS, this was not supported by neither the literature on this topic nor the data observed in the MTT assay. Alternatively, this result could be seen as a false positive result. Furthermore, an interference with the used testing kit is also possible. Therefore, a third viability test may be needed for confirmation of the result. It should also be noted that since 200 µM is far above the reported physiological peak concentrations of melatonin *in vivo*, the relevance of this concentration to physiological conditions is therefore limited.

Overall, excluding the decrease in viability with 200 µM of melatonin after 24 h of incubation using the ATP assay, melatonin presented reliable negative results, as expected. There were neither significant histologic changes nor further viability decreases in the PCLS. The lack of a reaction of PCLS to melatonin treatment demonstrates the reliability of PCLS in toxicological research.

4.4. Conclusion

Overall, the use of PCTS can increase the data gain per animal in scientific research. The tissue of one animal provides many PCTS that can be used in different experimental conditions. While there is a desire to reduce animal experiments, *in vitro* alternatives such as cell culture are insufficient to replace them. This necessitates research into *ex vivo* alternatives that lie somewhere between the two extremes, such as PCTS.

PCTS are not new and have already been used in different scientific settings. Their potential in toxicological research is also evident. Especially PCLS are already more advanced in terms of research and various toxins have already been tested on them.

In this thesis, PCLS proved to be reliably cultivatable under different incubation conditions, such as varying slice thicknesses and different medium compositions. PCHS were tested as well, but had significant challenges to them, mainly due to the small organ size of mice. Alternatively, PCHS from larger animals such as rats or pigs could be more useful. Initial experiments indicated positive effects on PCHS viability through the use of antioxidants in their culture media.

The treatment of PCLS with different compounds has shown that PCLS provide reliable results in toxicologic research. A dose-dependent decrease in viability was observed with acetaminophen and cisplatin treatment and a lack of response was observed with isoniazid and melatonin treatment. This is consistent with the responses to the compounds in an *in vivo* setting, and this can be seen as a proof of concept. The viability of PCLS can be assessed with similar assays as in cell cultures. In this thesis, it was found that ATP measurements were more sensitive to changes in viability, while more stable results were obtained with the MTT assay.

Right now, there are still some significant limitations to PCLS. The PCLS are not viable enough for the study of long-term and chronic toxic reactions. The PCLS were mainly suitable for short incubation periods and experiments in which the key data point was around 24 h of incubation. The PCLS had downregulated mRNAs for biotransformation enzymes and had shown early necrotic changes in histology. Therefore, further improvement in PCLS lifespan is desirable.

Nevertheless, PCTS are an important alternative to established laboratory methods. Further research in the field of PCTS should be conducted, as it may become an

important tool in the future.

5. Literature

1. Spruck C, Bousejra G, Erbay A, Herbrich S, Dimitriadis A, Röntgen Z, et al. Mouse precision-cut liver and kidney slices: an optimized ex vivo model for acute toxicity testing. bioRxiv. 2025:2025.07.21.665916.
2. U.S. Food and Drug Administration. Advancing Health Through Innovation: New Drug Therapy Approvals 2022. 2022.
3. Temple R. Current definitions of phases of investigation and the role of the FDA in the conduct of clinical trials. Am Heart J. 2000;139(4):S133-5.
4. Honek J. Preclinical research in drug development. Medical Writing. 2017;26(4).
5. U.S. Food and Drug Administration. The Drug Development Process - Step 2: Preclinical Research 2018 [Available from: https://www.fda.gov/patients/drug-development-process/step-2-preclinical-research.
6. European Commission. Summary Report on the statistics on the use of animals for scientific purposes in the Member States of the European Union and Norway in 2020. Brussels; 2023.
7. German Reference Centre for Ethics in the Life Sciences (DRZE). Animal Experiments in Research 2020 [Available from: https://www.drze.de/en/research-publications/in-focus/animal-experiments-in-research.
8. Russell WMS, Burch RL. The principles of humane experimental technique: Methuen; 1959.
9. Lewis DI. Animal experimentation: implementation and application of the 3Rs. Emerging Topics in Life Sciences. 2019;3(6):675-9.
10. Balls M, Combes R. Animal Experimentation and Alternatives: Revealed Preferences. Alternatives to Laboratory Animals. 2017;45(1):1-3.
11. Fernandes MR, Pedroso AR. Animal experimentation: A look into ethics, welfare and alternative methods. Rev Assoc Med Bras (1992). 2017;63(11):923-8.
12. National Centre for the Replacement Refinement and Reduction of Animals in Research. The 3Rs [Available from: https://www.nc3rs.org.uk/who-we-are/3rs.
13. Tee LF, Young JJ, Maruyama K, Kimura S, Suzuki R, Endo Y, et al. Electric shock causes a fleeing-like persistent behavioral response in the nematode Caenorhabditis elegans. Genetics. 2023;225(2).
14. Curzer HJ, Perry G, Wallace MC, Perry D. The Three Rs of Animal Research: What they Mean for the Institutional Animal Care and Use Committee and Why. Sci Eng Ethics. 2016;22(2):549-65.
15. Doke SK, Dhawale SC. Alternatives to animal testing: A review. Saudi Pharmaceutical Journal. 2015;23(3):223-9.
16. DeMello M. Animals and Society: An Introduction to Human-Animal Studies. New York Chichester, West Sussex: Columbia University Press; 2021.
17. Kiani AK, Pheby D, Henehan G, Brown R, Sieving P, Sykora P, et al. Ethical considerations regarding animal experimentation. J Prev Med Hyg. 2022;63(2 Suppl 3):E255-e66.
18. Balcombe J. Animal pleasure and its moral significance. Applied Animal Behaviour Science. 2009;118(3):208-16.
19. FDA Modernization Act 2.0, (2022).
20. Directive 2010/63/EU of the European Parliament and of the Council of 22 September 2010 on the protection of animals used for scientific purposes, (2010).
21. Saeidnia S, Manayi A, Abdollahi M. From in vitro Experiments to in vivo and Clinical Studies; Pros and Cons. Curr Drug Discov Technol. 2015;12(4):218-24.

22. Alsafadi HN, Staab-Weijnitz CA, Lehmann M, Lindner M, Peschel B, Konigshoff M, et al. An ex vivo model to induce early fibrosis-like changes in human precision-cut lung slices. Am J Physiol Lung Cell Mol Physiol. 2017;312(6):L896-L902.
23. de Graaf IA, Olinga P, de Jager MH, Merema MT, de Kanter R, van de Kerkhof EG, et al. Preparation and incubation of precision-cut liver and intestinal slices for application in drug metabolism and toxicity studies. Nat Protoc. 2010;5(9):1540-51.
24. Krumdieck CL, dos Santos J, Ho K-J. A new instrument for the rapid preparation of tissue slices. Analytical Biochemistry. 1980;104(1):118-23.
25. Dunn JC, Tompkins RG, Yarmush ML. Hepatocytes in collagen sandwich: evidence for transcriptional and translational regulation. Journal of Cell Biology. 1992;116(4):1043-53.
26. Parasuraman S. Toxicological screening. J Pharmacol Pharmacother. 2011;2(2):74-9.
27. Bruce RD. An up-and-down procedure for acute toxicity testing. Fundam Appl Toxicol. 1985;5(1):151-7.
28. Bhakuni GS, Bedi O, Bariwal J, Deshmukh R, Kumar P. Animal models of hepatotoxicity. Inflamm Res. 2016;65(1):13-24.
29. Tan TC, Scherrer-Crosbie M. Assessing the Cardiac Toxicity of Chemotherapeutic Agents: Role of Echocardiography. Curr Cardiovasc Imaging Rep. 2012;5(6):403-9.
30. Andersson TB. The application of HepRG cells in evaluation of cytochrome P450 induction properties of drug compounds. Methods Mol Biol. 2010;640:375-87.
31. Donato MT, Tolosa L, Gómez-Lechón MJ. Culture and Functional Characterization of Human Hepatoma HepG2 Cells. Methods Mol Biol. 2015;1250:77-93.
32. Pognan F, Beilmann M, Boonen HCM, Czich A, Dear G, Hewitt P, et al. The evolving role of investigative toxicology in the pharmaceutical industry. Nature Reviews Drug Discovery. 2023;22(4):317-35.
33. Blouin A, Bolender RP, Weibel ER. Distribution of organelles and membranes between hepatocytes and nonhepatocytes in the rat liver parenchyma. A stereological study. J Cell Biol. 1977;72(2):441-55.
34. Proctor WR, Foster AJ, Vogt J, Summers C, Middleton B, Pilling MA, et al. Utility of spherical human liver microtissues for prediction of clinical drug-induced liver injury. Arch Toxicol. 2017;91(8):2849-63.
35. Palma E, Doornebal EJ, Chokshi S. Precision-cut liver slices: a versatile tool to advance liver research. Hepatol Int. 2019;13(1):51-7.
36. Parrish AR, Gandolfi AJ, Brendel K. Precision-cut tissue slices: Applications in pharmacology and toxicology. Life Sciences. 1995;57(21):1887-901.
37. Starokozhko V, Greupink R, van de Broek P, Soliman N, Ghimire S, de Graaf IAM, et al. Rat precision-cut liver slices predict drug-induced cholestatic injury. Arch Toxicol. 2017;91(10):3403-13.
38. Vatakuti S, Olinga P, Pennings JLA, Groothuis GMM. Validation of precision-cut liver slices to study drug-induced cholestasis: a transcriptomics approach. Arch Toxicol. 2017;91(3):1401-12.
39. Hadi M, Dragovic S, van Swelm R, Herpers B, van de Water B, Russel FG, et al. AMAP, the alleged non-toxic isomer of acetaminophen, is toxic in rat and human liver. Arch Toxicol. 2013;87(1):155-65.
40. Hasuda AL, Person E, Khoshal AK, Bruel S, Puel S, Oswald IP, et al. Deoxynivalenol induces apoptosis and inflammation in the liver: Analysis using precision-cut liver slices. Food Chem Toxicol. 2022;163:112930.

41. Szalowska E, Pronk TE, Peijnenburg AA. Cyclosporin A induced toxicity in mouse liver slices is only slightly aggravated by Fxr-deficiency and co-occurs with upregulation of pro-inflammatory genes and downregulation of genes involved in mitochondrial functions. BMC Genomics. 2015;16:822.
42. Cao-Ehlker X, Fischer C, Lu K, Bruegmann T, Sasse P, Dendorfer A, et al. Optimized Conditions for the Long-Term Maintenance of Precision-Cut Murine Myocardium in Biomimetic Tissue Culture. Bioengineering. 2023;10(2):171.
43. Ou Q, Jacobson Z, Abouleisa RRE, Tang XL, Hindi SM, Kumar A, et al. Physiological Biomimetic Culture System for Pig and Human Heart Slices. Circ Res. 2019;125(6):628-42.
44. Meki MH, Miller JM, Mohamed TMA. Heart Slices to Model Cardiac Physiology. Front Pharmacol. 2021;12:617922.
45. Miller JM, Meki MH, Ou Q, George SA, Gams A, Abouleisa RRE, et al. Heart slice culture system reliably demonstrates clinical drug-related cardiotoxicity. Toxicol Appl Pharmacol. 2020;406:115213.
46. Trefts E, Gannon M, Wasserman DH. The liver. Current Biology. 2017;27(21):R1147-R51.
47. Kalra A, Yetiskul E, Wehrle CJ, Tuma F. Physiology, Liver. StatPearls. Treasure Island (FL): StatPearls Publishing

48. Crawford JM, Möckel GM, Crawford AR, Hagen SJ, Hatch VC, Barnes S, et al. Imaging biliary lipid secretion in the rat: ultrastructural evidence for vesiculation of the hepatocyte canalicular membrane. Journal of Lipid Research. 1996;36(10):2147-63.
49. Maldonado-Valderrama J, Wilde P, Macierzanka A, Mackie A. The role of bile salts in digestion. Adv Colloid Interface Sci. 2011;165(1):36-46.
50. Almazroo OA, Miah MK, Venkataramanan R. Drug Metabolism in the Liver. Clinics in Liver Disease. 2017;21(1):1-20.
51. Benedetti MS, Whomsley R, Poggesi I, Cawello W, Mathy F-X, Delporte M-L, et al. Drug metabolism and pharmacokinetics. Drug Metabolism Reviews. 2009;41(3):344-90.
52. Kruepunga N, Hakvoort TBM, Hikspoors JPJM, Köhler SE, Lamers WH. Anatomy of rodent and human livers: What are the differences? Biochimica et Biophysica Acta (BBA) - Molecular Basis of Disease. 2019;1865(5):869-78.
53. Kiernan F, Green JH. XXIX. The anatomy and physiology of the liver. Philosophical Transactions of the Royal Society of London. 1833;123:711-70.
54. Sasse D, Spornitz UM, Piotr Maly I. Liver Architecture. Enzyme and Protein. 1992;46(1-3):8-32.
55. Mall FP. A study of the structural unit of the liver. American Journal of Anatomy. 1906;5(3):227-308.
56. Rappaport AM, Borowy ZJ, Lougheed WM, Lotto WN. Subdivision of hexagonal liver lobules into a structural and functional unit. Role in hepatic physiology and pathology. The Anatomical Record. 1954;119(1):11-33.
57. Wünsche A. [Comparison of liver lobule types, including Rappaport's acinus in swine]. Anat Histol Embryol. 1985;14(1):15-32.
58. Jungermann K, Katz N. Functional specialization of different hepatocyte populations. Physiological Reviews. 1989;69(3):708-64.
59. Braeuning A, Ittrich C, Köhle C, Hailfinger S, Bonin M, Buchmann A, et al. Differential gene expression in periportal and perivenous mouse hepatocytes. The FEBS Journal. 2006;273(22):5051-61.
60. Gebhardt R. Metabolic zonation of the liver: Regulation and implications for liver function. Pharmacology & Therapeutics. 1992;53(3):275-354.

61. Lau C, Kalantari B, Batts KP, Ferrell LD, Nyberg SL, Graham RP, et al. The Voronoi theory of the normal liver lobular architecture and its applicability in hepatic zonation. Scientific Reports. 2021;11(1):9343.
62. Blouin A, Bolender RP, Weibel ER. Distribution of organelles and membranes between hepatocytes and nonhepatocytes in the rat liver parenchyma. A stereological study. Journal of Cell Biology. 1977;72(2):441-55.
63. Naito M, Hasegawa G, Takahashi K. Development, differentiation, and maturation of Kupffer cells. Microscopy Research and Technique. 1997;39(4):350-64.
64. Burt AD. C. L. Oakley Lecture (1993). Cellular and molecular aspects of hepatic fibrosis. J Pathol. 1993;170(2):105-14.
65. Hautekeete ML, Geerts A. The hepatic stellate (Ito) cell: its role in human liver disease. Virchows Archiv. 1997;430(3):195-207.
66. Aizarani N, Saviano A, Sagar, Mailly L, Durand S, Herman JS, et al. A human liver cell atlas reveals heterogeneity and epithelial progenitors. Nature. 2019;572(7768):199-204.
67. Park H-J, Choi J, Kim H, Yang D-Y, An TH, Lee E-W, et al. Cellular heterogeneity and plasticity during NAFLD progression. Frontiers in Molecular Biosciences. 2023;10.
68. Lee Y-T. The mediastinum. Gastrointestinal Endoscopy. 2009;69(2, Supplement):S81-S3.
69. Antonopoulos AS, Goliopoulou A, Vogiatzi G, Tousoulis D. Chapter 2.2 - Myocardial Oxygen Consumption. In: Tousoulis D, editor. Coronary Artery Disease: Academic Press; 2018. p. 127-36.
70. Institute of Medicine (US) Committee on Organ Procurement and Transplantation Policy. Organ Failure and Patient Survival. Organ Procurement and Transplantation: Assessing Current Policies and the Potential Impact of the DHHS Final Rule. Washington (DC): National Academies Press (US); 1999.
71. Carvajal C, Goyal A, Tadi P. Cardioplegia. StatPearls. Treasure Island (FL): StatPearls Publishing

72. Pinto AR, Ilinykh A, Ivey MJ, Kuwabara JT, D'Antoni ML, Debuque R, et al. Revisiting Cardiac Cellular Composition. Circulation Research. 2016;118(3):400-9.
73. Vasques F, Cavazza A, Bernal W. Acute liver failure. Current Opinion in Critical Care. 2022;28(2).
74. Babai S, Auclert L, Le-Louët H. Safety data and withdrawal of hepatotoxic drugs. Therapies. 2021;76(6):715-23.
75. McGill MR, Jaeschke H. Animal models of drug-induced liver injury. Biochim Biophys Acta Mol Basis Dis. 2019;1865(5):1031-9.
76. Fisher K, Vuppalanchi R, Saxena R. Drug-Induced Liver Injury. Archives of Pathology & Laboratory Medicine. 2015;139(7):876-87.
77. Albakri A. Drugs-related cardiomyopathy: A systematic review and pooled analysis of pathophysiology, diagnosis and clinical management. Internal Medicine and Care. 2019;3(1).
78. Page RL, 2nd, O'Bryant CL, Cheng D, Dow TJ, Ky B, Stein CM, et al. Drugs That May Cause or Exacerbate Heart Failure: A Scientific Statement From the American Heart Association. Circulation. 2016;134(6):e32-69.
79. Li S, Xu Z, Guo M, Li M, Wen Z. Drug-induced QT Prolongation Atlas (DIQTA) for enhancing cardiotoxicity management. Drug Discovery Today. 2022;27(3):831-7.

80. Nikles CJ, Yelland M, Del Mar C, Wilkinson D. The Role of Paracetamol in Chronic Pain: An Evidence-Based Approach. American Journal of Therapeutics. 2005;12(1):80-91.
81. Guggenheimer J, Moore PA. The therapeutic applications of and risks associated with acetaminophen use: a review and update. J Am Dent Assoc. 2011;142(1):38-44.
82. Graham GG, Scott KF. Mechanism of action of paracetamol. Am J Ther. 2005;12(1):46-55.
83. Bonnefont J, Courade JP, Alloui A, Eschalier A. [Antinociceptive mechanism of action of paracetamol]. Drugs. 2003;63 Spec No 2:1-4.
84. Ghanem CI, Pérez MJ, Manautou JE, Mottino AD. Acetaminophen from liver to brain: New insights into drug pharmacological action and toxicity. Pharmacol Res. 2016;109:119-31.
85. Lee KK, Imaizumi N, Chamberland SR, Alder NN, Boelsterli UA. Targeting mitochondria with methylene blue protects mice against acetaminophen-induced liver injury. Hepatology. 2015;61(1):326-36.
86. Cai X, Cai H, Wang J, Yang Q, Guan J, Deng J, et al. Molecular pathogenesis of acetaminophen-induced liver injury and its treatment options. J Zhejiang Univ Sci B. 2022;23(4):265-85.
87. Jaeschke H, McGill MR, Ramachandran A. Oxidant stress, mitochondria, and cell death mechanisms in drug-induced liver injury: lessons learned from acetaminophen hepatotoxicity. Drug Metab Rev. 2012;44(1):88-106.
88. Jaeschke H, Xie Y, McGill MR. Acetaminophen-induced Liver Injury: from Animal Models to Humans. J Clin Transl Hepatol. 2014;2(3):153-61.
89. Ntamo Y, Ziqubu K, Chellan N, Nkambule BB, Nyambuya TM, Mazibuko-Mbeje SE, et al. Drug-Induced Liver Injury: Clinical Evidence of N-Acetyl Cysteine Protective Effects. Oxid Med Cell Longev. 2021;2021:3320325.
90. Ghosh S. Cisplatin: The first metal based anticancer drug. Bioorganic Chemistry. 2019;88:102925.
91. Ciarimboli G. Membrane transporters as mediators of Cisplatin effects and side effects. Scientifica (Cairo). 2012;2012:473829.
92. Kanno Y, Chen CY, Lee HL, Chiou JF, Chen YJ. Molecular Mechanisms of Chemotherapy Resistance in Head and Neck Cancers. Front Oncol. 2021;11:640392.
93. Kiss RC, Xia F, Acklin S. Targeting DNA Damage Response and Repair to Enhance Therapeutic Index in Cisplatin-Based Cancer Treatment. International Journal of Molecular Sciences. 2021;22(15):8199.
94. Waseem M, Bhardwaj M, Tabassum H, Raisuddin S, Parvez S. Cisplatin hepatotoxicity mediated by mitochondrial stress. Drug and Chemical Toxicology. 2015;38(4):452-9.
95. Lu Y, Cederbaum AI. Cisplatin-Induced Hepatotoxicity Is Enhanced by Elevated Expression of Cytochrome P450 2E1. Toxicological Sciences. 2005;89(2):515-23.
96. Hartman JH, Miller GP, Meyer JN. Toxicological Implications of Mitochondrial Localization of CYP2E1. Toxicol Res (Camb). 2017;6(3):273-89.
97. Yakes FM, Van Houten B. Mitochondrial DNA damage is more extensive and persists longer than nuclear DNA damage in human cells following oxidative stress. Proceedings of the National Academy of Sciences. 1997;94(2):514-9.
98. Heifets LB, Lindholm-Levy PJ, Flory M. Comparison of bacteriostatic and bactericidal activity of isoniazid and ethionamide against Mycobacterium avium and Mycobacterium tuberculosis. Am Rev Respir Dis. 1991;143(2):268-70.
99. Vilchèze C, William R. Jacobs J. The Mechanism of Isoniazid Killing: Clarity Through the Scope of Genetics. Annual Review of Microbiology. 2007;61(1):35-50.

100. Boelsterli UA, Lee KK. Mechanisms of isoniazid-induced idiosyncratic liver injury: Emerging role of mitochondrial stress. Journal of Gastroenterology and Hepatology. 2014;29(4):678-87.
101. Preece NE, Ghatineh S, Timbrell JA. Course of ATP depletion in hydrazine hepatotoxicity. Archives of Toxicology. 1990;64(1):49-53.
102. Lee KK, Fujimoto K, Zhang C, Schwall CT, Alder NN, Pinkert CA, et al. Isoniazid-induced cell death is precipitated by underlying mitochondrial complex I dysfunction in mouse hepatocytes. Free Radical Biology and Medicine. 2013;65:584-94.
103. Rungemorris M, Wu N, Novak RF. Hydrazine-Mediated DNA Damage: Role of Hemoprotein, Electron Transport, and Organic Free Radicals. Toxicology and Applied Pharmacology. 1994;125(1):123-32.
104. Metushi IG, Nakagawa T, Uetrecht J. Direct Oxidation and Covalent Binding of Isoniazid to Rodent Liver and Human Hepatic Microsomes: Humans Are More Like Mice than Rats. Chemical Research in Toxicology. 2012;25(11):2567-76.
105. Metushi IG, Zhu X, Chen X, Gardam MA, Uetrecht J. Mild Isoniazid-Induced Liver Injury in Humans Is Associated with an Increase in Th17 Cells and T Cells Producing IL-10. Chemical Research in Toxicology. 2014;27(4):683-9.
106. Metushi IG, Sanders C, Group TALS, Lee WM, Uetrecht J. Detection of anti-isoniazid and anti–cytochrome P450 antibodies in patients with isoniazid-induced liver failure. Hepatology. 2014;59(3):1084-93.
107. Claustrat B, Leston J. Melatonin: Physiological effects in humans. Neurochirurgie. 2015;61(2):77-84.
108. Cardinali DP, Pévet P. Basic aspects of melatonin action. Sleep Medicine Reviews. 1998;2(3):175-90.
109. Reiter RJ, Mayo JC, Tan D-X, Sainz RM, Alatorre-Jimenez M, Qin L. Melatonin as an antioxidant: under promises but over delivers. Journal of Pineal Research. 2016;61(3):253-78.
110. Zhang JJ, Meng X, Li Y, Zhou Y, Xu DP, Li S, et al. Effects of Melatonin on Liver Injuries and Diseases. Int J Mol Sci. 2017;18(4).
111. Guo P, Pi H, Xu S, Zhang L, Li Y, Li M, et al. Melatonin Improves Mitochondrial Function by Promoting MT1/SIRT1/PGC-1 Alpha-Dependent Mitochondrial Biogenesis in Cadmium-Induced Hepatotoxicity In Vitro. Toxicological Sciences. 2014;142(1):182-95.
112. Kanno S, Tomizawa A, Hiura T, Osanai Y, Kakuta M, Kitajima Y, et al. Melatonin protects on toxicity by acetaminophen but not on pharmacological effects in mice. Biol Pharm Bull. 2006;29(3):472-6.
113. Aldini G, Altomare A, Baron G, Vistoli G, Carini M, Borsani L, et al. N-Acetylcysteine as an antioxidant and disulphide breaking agent: the reasons why. Free Radical Research. 2018;52(7):751-62.
114. Balsamo R, Lanata L, Egan CG. Mucoactive drugs. Eur Respir Rev. 2010;19(116):127-33.
115. Whitehouse LW, Wong LT, Paul CJ, Pakuts A, Solomonraj G. Postabsorption antidotal effects of N-acetylcysteine on acetaminophen-induced hepatotoxicity in the mouse. Can J Physiol Pharmacol. 1985;63(5):431-7.
116. Samuni Y, Goldstein S, Dean OM, Berk M. The chemistry and biological activities of N-acetylcysteine. Biochimica et Biophysica Acta (BBA) - General Subjects. 2013;1830(8):4117-29.
117. Ciriminna R, Pagliaro M. Industrial Oxidations with Organocatalyst TEMPO and Its Derivatives. Organic Process Research & Development. 2010;14(1):245-51.

118. Luo Z, Chen Y, Chen S, Welch WJ, Andresen BT, Jose PA, et al. Comparison of inhibitors of superoxide generation in vascular smooth muscle cells. Br J Pharmacol. 2009;157(6):935-43.
119. Wilcox CS, Pearlman A. Chemistry and antihypertensive effects of tempol and other nitroxides. Pharmacol Rev. 2008;60(4):418-69.
120. Mosmann T. Rapid colorimetric assay for cellular growth and survival: Application to proliferation and cytotoxicity assays. Journal of Immunological Methods. 1983;65(1):55-63.
121. Kumar P, Nagarajan A, Uchil PD. Analysis of Cell Viability by the MTT Assay. Cold Spring Harb Protoc. 2018;2018(6).
122. Spinner DM. MTT growth assays in ovarian cancer. Methods Mol Med. 2001;39:175-7.
123. Hui L, Gao S, Liu T, Cao C, Guo J, Hao R, et al. [Evaluation of vitro hepatotoxicity of monocrotaline by precision-cut liver slice technique]. Zhongguo Zhong Yao Za Zhi. 2011;36(5):628-32.
124. Obatomi DK, Brant S, Anthonypillai V, Early DA, Bach PH. Optimizing preincubation conditions for precision-cut rat kidney and liver tissue slices: effect of culture media and antioxidants. Toxicol In Vitro. 1998;12(6):725-37.
125. Präbst K, Engelhardt H, Ringgeler S, Hübner H. Basic Colorimetric Proliferation Assays: MTT, WST, and Resazurin. In: Gilbert DF, Friedrich O, editors. Cell Viability Assays: Methods and Protocols. New York, NY: Springer New York; 2017. p. 1-17.
126. Lomakina GY, Modestova YA, Ugarova NN. Bioluminescence assay for cell viability. Biochemistry (Moscow). 2015;80(6):701-13.
127. Smale ST. Luciferase assay. Cold Spring Harb Protoc. 2010;2010(5):pdb.prot5421.
128. Feldman AT, Wolfe D. Tissue processing and hematoxylin and eosin staining. Methods Mol Biol. 2014;1180:31-43.
129. Chan JKC. The Wonderful Colors of the Hematoxylin–Eosin Stain in Diagnostic Surgical Pathology. International Journal of Surgical Pathology. 2014;22(1):12-32.
130. Appelboom JWT, Brodsky WA, Rehm WS. The Concentration of Glucose in Mammalian Liver. Journal of General Physiology. 1959;43(2):467-79.
131. Chen QM, Maltagliati AJ. Nrf2 at the heart of oxidative stress and cardiac protection. Physiological Genomics. 2018;50(2):77-97.
132. Prins GH, Rios-Morales M, Gerding A, Reijngoud DJ, Olinga P, Bakker BM. The Effects of Butyrate on Induced Metabolic-Associated Fatty Liver Disease in Precision-Cut Liver Slices. Nutrients. 2021;13(12).
133. Starokozhko V, Abza GB, Maessen HC, Merema MT, Kuper F, Groothuis GM. Viability, function and morphological integrity of precision-cut liver slices during prolonged incubation: Effects of culture medium. Toxicol In Vitro. 2015;30(1 Pt B):288-99.
134. Thiele GM, Duryee MJ, Thiele GE, Tuma DJ, Klassen LW. Review: Precision Cut Liver Slices for the Evaluation of Fatty Liver and Fibrosis. Curr Mol Pharmacol. 2017;10(3):249-54.
135. Granitzny A, Knebel J, Schaudien D, Braun A, Steinberg P, Dasenbrock C, et al. Maintenance of high quality rat precision cut liver slices during culture to study hepatotoxic responses: Acetaminophen as a model compound. Toxicology in Vitro. 2017;42:200-13.
136. Dewyse L, De Smet V, Verhulst S, Eysackers N, Kunda R, Messaoudi N, et al. Improved Precision-Cut Liver Slice Cultures for Testing Drug-Induced Liver Fibrosis. Front Med (Lausanne). 2022;9:862185.

137. Huet O, Petit JM, Ratinaud MH, Julien R. NADH-dependent dehydrogenase activity estimation by flow cytometric analysis of 3-(4,5-dimethylthiazolyl-2-yl)-2,5-diphenyltetrazolium bromide (MTT) reduction. Cytometry. 1992;13(5):532-9.
138. Shi DY, Xie FZ, Zhai C, Stern JS, Liu Y, Liu SL. The role of cellular oxidative stress in regulating glycolysis energy metabolism in hepatoma cells. Mol Cancer. 2009;8:32.
139. Wu X, Roberto JB, Knupp A, Kenerson HL, Truong CD, Yuen SY, et al. Precision-cut human liver slice cultures as an immunological platform. J Immunol Methods. 2018;455:71-9.
140. Majno G, Joris I. Apoptosis, oncosis, and necrosis. An overview of cell death. Am J Pathol. 1995;146(1):3-15.
141. Celton-Morizur S, Desdouets C. Polyploidization of liver cells. Adv Exp Med Biol. 2010;676:123-35.
142. Greenbaum D, Colangelo C, Williams K, Gerstein M. Comparing protein abundance and mRNA expression levels on a genomic scale. Genome Biol. 2003;4(9):117.
143. Yang J, Liao M, Shou M, Jamei M, Yeo KR, Tucker GT, et al. Cytochrome p450 turnover: regulation of synthesis and degradation, methods for determining rates, and implications for the prediction of drug interactions. Curr Drug Metab. 2008;9(5):384-94.
144. Lupp A, Danz M, Müller D. Morphology and cytochrome P450 isoforms expression in precision-cut rat liver slices. Toxicology. 2001;161(1):53-66.
145. Olinga P, Groothuis GMM. Use of Human Tissue Slices in Drug Targeting Research. Drug Targeting2001. p. 309-31.
146. Yue J, Wang P, Liu YH, Wu JY, Chen J, Peng RX. Fast evaluation of oxidative DNA damage by liquid chromatography-electrospray tandem mass spectrometry coupled with precision-cut rat liver slices. Biomed Environ Sci. 2007;20(5):386-91.
147. Prins GH, Luangmonkong T, Oosterhuis D, Mutsaers HAM, Dekker FJ, Olinga P. A Pathophysiological Model of Non-Alcoholic Fatty Liver Disease Using Precision-Cut Liver Slices. Nutrients. 2019;11(3).
148. Simon E, Motyka M, Prins GH, Li M, Rust W, Kauschke S, et al. Transcriptomic profiling of induced steatosis in human and mouse precision-cut liver slices. Sci Data. 2023;10(1):304.
149. Kuhn UD, Splinter FK, Rost M, Müller D. Induction of cytochrome P450 1A1 in rat liver slices by 7-ethoxycoumarin and 4-methyl-7-ethoxycoumarin. Experimental and Toxicologic Pathology. 1998;50(4):491-6.
150. Jakubczyk K, Dec K, Kałduńska J, Kawczuga D, Kochman J, Janda K. Reactive oxygen species - sources, functions, oxidative damage. Pol Merkur Lekarski. 2020;48(284):124-7.
151. Minasian SM, Galagudza MM, Dmitriev YV, Kurapeev DI, Vlasov TD. Myocardial protection against global ischemia with Krebs-Henseleit buffer-based cardioplegic solution. J Cardiothorac Surg. 2013;8:60.
152. Ross AJ, Krumova I, Tunc B, Wu Q, Wu C, Camelliti P. A novel method to extend viability and functionality of living heart slices. Front Cardiovasc Med. 2023;10:1244630.
153. Lohmann J, Lessing U, Schriewer H, Clemens M, Gerlach U. The influence of paracetamol on the hepatic biosynthesis of lecithin. Arch Toxicol Suppl. 1984;7:236-9.
154. McGill MR, Williams CD, Xie Y, Ramachandran A, Jaeschke H. Acetaminophen-induced liver injury in rats and mice: comparison of protein adducts, mitochondrial dysfunction, and oxidative stress in the mechanism of toxicity. Toxicol Appl Pharmacol. 2012;264(3):387-94.

155. Jemnitz K, Veres Z, Monostory K, Kóbori L, Vereczkey L. Interspecies differences in acetaminophen sensitivity of human, rat, and mouse primary hepatocytes. Toxicol In Vitro. 2008;22(4):961-7.
156. Jackson CH, MacDonald NC, Cornett JW. Acetaminophen: a practical pharmacologic overview. Can Med Assoc J. 1984;131(1):25-32, 7.
157. Bhushan B, Apte U. Regeneration and Recovery after Acetaminophen Hepatotoxicity. Livers. 2023;3(2):300-9.
158. Salama B, El-Sherbini ES, El-Sayed G, El-Adl M, Kanehira K, Taniguchi A. The Effects of TiO(2) Nanoparticles on Cisplatin Cytotoxicity in Cancer Cell Lines. Int J Mol Sci. 2020;21(2).
159. Vakkuri O, Leppäluoto J, Kauppila A. Oral administration and distribution of melatonin in human serum, saliva and urine. Life Sci. 1985;37(5):489-95.

Acknowledgments

This thesis would not have been possible without the guidance and help of my supervisor, Professor Dr. Nicole Schupp. I would like to thank her unwavering support throughout my research journey. Her commitment to academic excellence and her attention to detail shaped this dissertation.

I am also thankful for my colleagues at the Institute of Toxicology for being great people in and out of the lab. Their collaboration, encouragement, and good humor made both the scientific work and the everyday life in the lab truly enjoyable. They created an inspiring and supportive environment that I will always cherish.

I would also like to extend my thanks to my family and friends. Their constant support gave me the strength to persevere during the most challenging phases of my journey. Without them, this work would not have been possible.